537.226 + 620 178.7 + 535.8

OPTICAL STUDY OF THE CHARACTERISTICS OF SHOCK-COMPRESSED CONDENSED DIELECTRICS

S. B. KORMER

Usp. Fiz. Nauk 94, 641–687 (April, 1964)

CONTENTS

INTRODUCTION

THE dynamic method of producing and measuring high pressures, developed in the post-war period (see surveys[1-3]), makes it possible to study the characteristics of condensed substances. Initially, the main purpose of these investigations was the determination of shock adiabats of substances having normal and lowered density and of their isentropic compressibility, knowledge of which would permit us to develop the equation of state for the substance at high densities, pressures, and temperatures[4-17], using some model considerations from the theory of the solid state. Research was done primarily on metals, for which in the very first works the range of pressures reached hundreds of thousands[5] and millions of bars[6]. By this method data have now been assembled for scores of elements and compounds over a very wide range of pressures up to 10 Mbar.[12,14,18] The trend toward the maximum possible limits brings about the problem of replacing the original chemical explosives by nuclear explosives[19,20], which would generate pressures of the order of several hundred megabars, and bring us nearer to that region where the conclusions of the quantum-statistical Thomas-Fermi model[21,22] become valid. Owing to the studies of polymorphic transformations at high pressures and temperatures, which led to the synthesis of artificial diamonds, the progress in high-pressure physics has become known to wide circles of nonspecialists. Under dynamic conditions this transformation[1] is 10^7–10^{14} times faster than when static pressure is applied. Considerable interest has thus arisen in the chemistry of ultrahigh pressures[23,24], which is already making its first strides.[25-28]

Investigation of substance transformations and their accomplishment lead to an interest in the kinetics of processes occurring during shock compression at the shock front; this compression is remarkable in many ways. Within a layer only several tens of interatomic spacings thick a considerable part of the kinetic energy supplied to the substance under shock compression is converted irreversibly into heat; the entropy, pressure, density, and temperature all change from their initial values to the ultimate ones, many times greater. The shock wave is a powerful generator of defects, formed during the strong plastic deformation taking place at the

wave front. These disturbances of the ideal crystal lattice, as under normal conditions, determine to a large extent the electrical, optical, and other physical characteristics of the material. The generation of imperfections brings about an acceleration of phase transformations [29,20,30] and is the reason for the relatively high conductivity, the absorbing power [30], and possibly the polarization of shock-compressed dielectrics reported by a number of investigators. [31-41]

All this stimulates interest in the study of processes taking place at the front of the shock wave. There is particular interest in optical methods that use a light beam as a laboratory instrument. These methods enable us to record changes of state in layers whose thickness is of the order of one-hundredth of the wavelength of light, inaccessible to any other method used in the study of fast phenomena.

The particular features of the optical method made it possible [42-45] to establish experimentally that, under shock compression, the density jump in the condensed substances takes place within a layer $\leq 10^{-6}$ cm thick and requires only $\tau \approx 10^{-12}$ sec. This period is comparable to that of the establishment of equilibrium in a phonon-phonon interaction. It has been found that the front of the shock wave is very smooth (mirrorlike), the roughness being considerably less than 10^{-6} cm. [42] Irregularities of the order of 10^{-5} cm have been reported at the front of a shock wave caused by the detonation of a liquid explosive [46,47]. Investigations of the reflection and refraction of light incident on the shock-compressed material showed [42-45] that the refractive index of both liquid and solid substances increases linearly with the density in a wide density range up to $\rho \approx 2\rho_0$, where ρ_0 is the density at atmospheric pressure. The proportionality factor is nearly the same as at atmospheric pressure. An anomalously high reflectivity of the shock front has been found [45] in carbon tetrachloride when its density becomes 1.9 times the normal value. Liquefaction of ionic crystals in the compressed state causes [43] a rise in the refractive index as well as in its derivative (by a factor of about 1.5—1.7), whereas at atmospheric pressure the same change of state is accompanied by a drop in the refractive index. These two facts are due to different variations of the refractive index with density in the liquid and solid phases of the material, and in turn to a change in the character of the interionic interaction on melting. The high sensitivity of the optical method to the density gradient [43] made it possible to reveal the structure of the shock front in substances that undergo polymorphic transformation. Thus, in the case of KCl and KBr, which undergo phase transition at 20 kbar, [48,16] it has been found [43] that the first phase existed at 100 kbar over a period of about 10^{-11}—10^{-12} sec. The same time was found in [44] for the transition of glass (heavy flint) into the plastic state at pressures exceeding 260 kbar. Below this pressure the state of the glass is initially described by a nonequilibrium adiabat of elastic compression. The transition into plastic state has a relaxational character.

Research on the optical characteristics of water with stepwise application of pressures between 20 and 40 kbar revealed [176] the phase transformation of water into ice VII. It is interesting that, when the pressure is applied dynamically, water freezes up within about 10^{-7} sec.

Some valuable information about the characteristics of various substances was supplied by investigating their radiation under shock compression. The rise in the brightness of radiation as the shock wave propagates in a body made it possible to determine [49,30] the absorption coefficients of shock-compressed ionic crystals at high temperatures. The absorption coefficients found under these conditions are about 100 times the normal values. Studies in the Soviet Union [50,15] and in the United States [51,20] have shown that the conductivity of dielectrics behind the shock front increases by a factor of more than 10^{10} times. Analysis of the absorption and conductivity characteristics of shock-compressed ionic crystals led to the conclusion [30] that the shock wave transforms the dielectric into a semiconductor with donor levels whose thermal ionization produces free electrons in the conduction band. According to this mechanism, the relatively high concentration of free electrons (10^{18} cm^{-3}) determines both the absorption power of shock-compressed ionic crystals and their conductivity [30].

Thermodynamic equilibrium in condensed materials is established much faster than in shock-compressed gases (approximately in inverse proportion to the densities). The relatively high absorption power of shock-compressed condensed dielectrics [49,30] and the short periods (about 10^{-9} sec) in which electrons manage to pass into the conduction band and reach equilibrium with the lattice [30], make it possible to measure them in certain ranges of temperature in shock-heated materials [49]. The important result of this work was the construction of the fusion curves for many ionic crystals up to record high pressures of the order of 0.5—2.5 Mbar; only the initial positions of the curves, up to 20—40 kbar, were previously known. While in many respects the high pressures attained by shock compression cannot fully replace static compression, since the density and the temperature are varying together, in the case of studies on the melting of materials nature itself supports the investigator. By changing the pressure we change the temperature and, in a certain pressure range, the states observed on the dynamic adiabat represent a section of the fusion curve [48].

When ionic crystals are compressed by a factor of 1.7, they remain solid up to a temperature of about 4000°K [49], which exceeds the melting point of the most refractory metals. Analysis of experimental data has shown that the entropy jump during fusion in the compressed state is close to that at atmospheric pressure. The heat of fusion in the compressed state is thus proportional to the melting temperature [49]. In contrast, the volume changes in the melting of ionic crystals compressed by a factor of 1.5—2 are smaller by approximately an order of magnitude than the volume change associated with melting at atmospheric pressure. The part played by the anharmonic nature of the oscillations has been determined, and it has been shown [49] that this has little influence on the heat capacity of solids up to melting temperatures of about 4000°K ($\Delta c_V/c_V \leq 10\%$).

At the same time, the heat capacity of an organic compound, lucite, increases substantially with rising

temperature. Further pressure increase during shock-compression of lucite causes far-reaching breakage of chemical bonds[52]. Changes in the phase states have been found on dynamic loading of carbon tetrachloride.

Nonequilibrium radiation many times stronger than thermal radiation has been found in a number of ionic crystals compressed at relatively low pressures (of the order of several hundred kbar). Thus, in the case of LiF at 340 kbar the measured light flux exceeds the expected equilibrium value by a factor of 10^{17}. Another form of nonequilibrium radiation was found when ionic crystals were shock-compressed with pressures of 2—5 Mbar. In these conditions, the radiation brightness was much lower than would correspond to the equilibrium temperature. Brightness temperatures differ increasingly from calculated values as the width of the energy gap is reduced. This effect is attributed to a screening of the equilibrium radiation by frontlayers of the shock-compressed material, in which the electron temperature has not yet reached its equilibrium level.

Our survey reports the main results obtained in studies of the optical characteristics of shock-compressed dielectrics and their temperatures behind the shock front. Some attention is paid to the methods of investigation and to their principles, since the literature (particularly foreign literature) does not as yet reflect any consensus as to the possibilities of optical methods in the research on shock-compressed materials, as a result of which the number of publications dealing with this subject is very limited. Most of the results described in our survey were obtained in the author's laboratory between 1956 and 1966. The results of some very extensive studies on the optical characteristics of statically compressed dielectrics have already been reviewed[53-55], and we shall not dwell on them here. We also omit consideration of the methods of obtaining and measuring pressures and densities under dynamic loading, including the optical methods, indispensable as they are for analysis of any other characteristics. These questions are adequately discussed in[1-3,20,54].

I. STUDY OF THE OPTICAL CHARACTERISTICS OF SHOCK-COMPRESSED CONDENSED MATERIALS, AND OF THE STRUCTURE AND SMOOTHNESS OF THE FRONTS OF LARGE-AMPLITUDE SHOCK WAVES

1. Experimental Procedure

Propagation of a strong shock wave through a material is accompanied by a rise in the latter's density and temperature and by a change in other characteristics, including optical ones. The change in density alone increases the refractive index and causes optical inhomogeneity of the medium, and this is the basis of many methods used for the optical recording of processes accompanied by shock waves.

The optical characteristics, and in particular the reflectivity of the shock front, are related to its surface texture and thickness. The high sensitivity of the reflectivity to the density gradient was first utilized by Hornig and his co-workers[56,57] for investigating the structure of the shock wave and detonation front in gases. Hornig et al. also studied the structure of shock waves in liquids at pressures of only a few atmospheres[58].

Knowledge of the reflectivity of shock-wave fronts in condensed media is also important for the determination of the emissivity of shock-heated substances when the latter's temperature is determined from their radiation (for further details see Sec. 7). For exactly this purpose, the present writer suggested in 1957 an investigation of the reflectivity of shock-compressed substances. This method, developed in collaboration with Yushko, Sinitsyn, and Krishkevich[42-45,176], was later applied to investigations of a wide range of phenomena. The success of these studies was greatly aided by the participation of Zel'dovich.

In[42-45,176] the light reflected from the shock front was recorded after passing through a layer of uncompressed originally transparent material as the wave moved through this layer. The principle is shown in Fig. 1. If the investigated material remains transparent after it has been compressed by the shock wave, it is possible to determine the refractive index of the com-

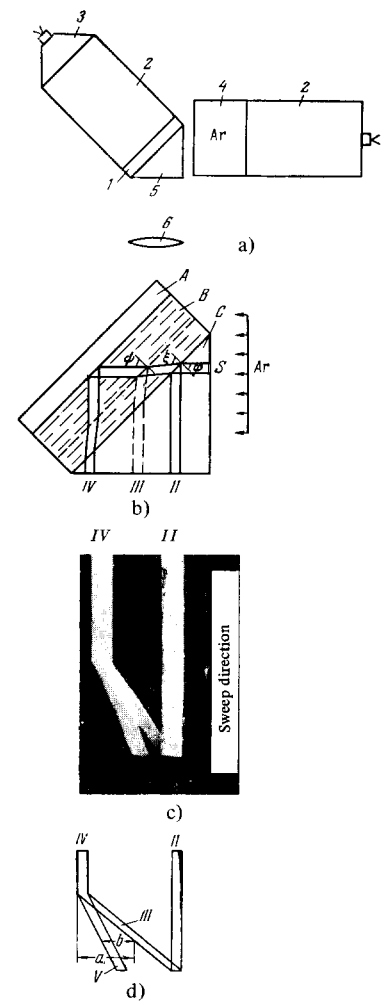

FIG. 1. Schematic diagram (a,b) and results (c,d) of an experiment on the measurement of the refractive index of a shock-compressed material and of the reflectivity of the shock front:

II, IV – light reflection from stationary boundaries B-C and A-B; III, V – light reflection from the shock front and moving boundary A-B; 1 – investigated material: 2,3 – explosive charges; 4 – explosive light source; 5 – prism; 6 – high-speed moving-image camera.

pressed material from the course of the rays. Use is made of the following relationship:

$$\frac{n_3^2 - n_1^2 \sin^2\varphi}{n_2^2 - n_1^2 \sin^2\varphi} = \frac{\mu}{\sigma}, \quad (1)$$

where φ is the angle of incidence, n_1, n_2, and n_3 are the refractive indices in the prism and in the investigated material before and after compression, and $\mu = a/b$ (see Fig. 1,d). The shock-front thickness has no effect on the refractive index obtained by this method, since the front is very thin compared to the compressed layer. This method is much less accurate ($\Delta n/n_0 \approx 1-2\%$) than the usual methods applied in refractive-index measurements, but it does provide an opportunity to find the refractive index of a material compressed by a factor of 1.5 to 2, and also gives a picture of the relationship between refractive index and density over a very much wider range of densities. Moreover, the accuracy of the method can be improved. Thus, in a recently published paper[59] the refractive indices of shock-compressed liquids were determined accurately to three decimal places.

The layout shown in Fig. 1 also makes it possible to determine the reflectivity of the shock front. It is only necessary to compare the intensity of a light beam reflected from the shock front with the intensity of an identical beam reflected from an optical boundary having a known reflectivity. The optical boundary between the investigated material and the prism is used as the reference surface (boundary B-C).

The reflection coefficient of the shock wave front can be found from:

$$R_{s.w} = \frac{I_{s.w}}{I_{ref}} \frac{R_{ref}(\varphi)}{[1 - R_{ref}(\varphi)]^2}; \quad (2)$$

where $I_{S.W.}/I_{ref}$ is the ratio of the intensities reflected from the shock front and from the reference surface, found from the blackening of film by a photometric method, and $R_{ref}(\varphi)$ is the reflection coefficient of the reference surface.

If unpolarized light is used, formula (2) can only be regarded as approximate. The resolution of this method under the conditions of an explosion experiment, when the investigated material is 10 to 15 m from the recording instrument, is $R \geq 10^{-3}$. The error of a single measurement is $\Delta R/R \approx \pm(5 - 10)\%$.

The distinguishing features of an explosion experiment and the relatively low brightness of available light sources made it in many cases impossible to carry out spectral measurements. For this reason the investigation was carried out on materials having low dispersion in the visible spectrum.

The above methods were employed in studies of the optical characteristics of both solid and liquid initially transparent dielectrics. The pressure in the investigated body was varied by varying the detonation power of the explosive, and also by generating a shock wave in it by impact of plates of various materials driven by an explosion[7,15,16,49].

The state of shock-compressed material may be assessed from the propagation velocity of a shock wave within it, which is determined in the same experiment.

Future increases in the brightness of the external light source may permit spectral measurements of the change in the dispersion of the material's refractive index under compression, and determination of the edge of the absorption band. Such measurements may shed light on the changes in the electronic structure of condensed dielectrics and on their transformation into the metallic state. Thus, the present studies of Drickamer et al.[54,55,19] with static compression might be extended to a much wider range of densities. A promising method for this work would be based on light reflection when a powerful shock wave is started not by explosion but by the impact of a plate accelerated in a hydrogen or helium gun[60]. The recording apparatus could then be brought substantially nearer to the investigated specimen and, if the brightness of the external light source were simultaneously raised as well, the accuracy and resolution of the method would be greatly enhanced.

2. Front Thickness and Smoothness of Shock Waves in Condensed Inert and Explosive Substances

In an idealized model the shock-wave front in the condensed material is regarded as an infinitely thin boundary surface between matter at rest and matter in motion. In fact, viscosity and thermal conduction result in a finite thickness of the shock front. In optical investigations in which light is reflected from the sections with the highest dn/dx, it may be useful to define the thickness of the transition layer as

$$\Delta x = \frac{\Delta n}{(dn/dx)_{max}} \equiv \frac{\Delta \rho}{(d\rho/dx)_{max}}. \quad (3)$$

Since ρ and n behave in an identical manner, the variations of reflectivity may be directly related to the density variations. We note that the right side of (3) is the same as Prandtl's definition of the shock-front thickness. Following[58] and[61], the front thickness in liquids at very low shock-wave amplitudes, of the order of a few tens of atmospheres, is 10^{-4} cm. It is known[62,2] that the greater the shock wave intensity, i.e., the greater the pressure jump, the thinner the front.

However, up to now there have been no experimental studies providing a resolution better than 10^{-2} cm (see[29]). This gap was filled when the light-reflection method came into use. Estimates have shown that, for a transition-layer profile as in[63], the incident light is reflected in accordance with Fresnel's law when $L/\lambda \leq 10^{-2}$, which for $\lambda = 5 \times 10^{-5}$ cm gives $L \leq 5 \times 10^{-7}$ cm. When $L \leq 5 \times 10^{-6}$ cm $\approx \lambda/2\pi$, practically no light will be reflected from the optical boundary. This makes it possible to resolve front spreading of the order of 10^{-6} cm, which is quite beyond the reach of other methods.

The materials chosen for the first investigations in[45] were glycerol, ethyl alcohol, and water, which all remain sufficiently transparent behind the shock front at pressures up to 100–300 kbar. This made it possible to compare the refractive index determined directly from the course of the beam in the compressed material (when the transition layer has no effect on the measurement[42]) with the refractive index n_F calculated by Fresnel's equations from the experimentally found reflection coefficient. Both for glycerol and ethanol (Fig. 2) the two refractive indices were approximately equal within the limits of experimental accuracy. This means that the density jump at the shock front occurs within a layer at the most 100 Å thick in a time of the

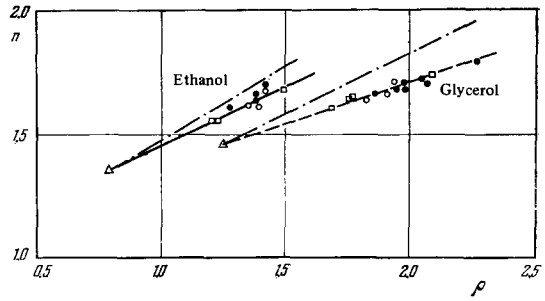

FIG. 2. Relationship between the refractive index and density in ethanol and glycerol[45,59]. Calculated by the Lorenz-Lorentz formula (6) (—·—) and by (9) (—, – –). The experimental data were obtained by the photometric method in [45] (●) and by the geometric method in [45] (○) and [59] (□).

order of 10^{-12} sec. The same conclusion can be drawn from measurements of the reflectivity at the shock front in toluene (P = 170 kbar, σ = 1.76) at various angles of incidence. The completely satisfactory agreement between experimental results (Fig. 3) and Fresnel's equations indicates a sharp jump of density at the shock front. Similar results were obtained for benzene and lucite. Investigations of ionic crystals (Sec. 4) also lead to the conclusion that the profile of the shock wave is just as steep.

The results obtained in shock compression of water[42] (Fig. 4) constitute an exception; the refractive indices were in this case found by photometric means, beginning from σ ≈ 1.6 (P ≈ 90 kbar), and were found to be somewhat lower than those obtained by the geometric method. This can obviously be attributed to the finite thickness of the transition layer in which the water was compressed. The water viscosity produces under normal conditions a front thickness that should not cause any noticeable deviations from Fresnel's equations. The photometric data can be explained[42] if it is assumed[64] that the viscosity of water increases greatly when the pressure reaches P_{cr} = 60—80 kbar. In these circumstances, when the shock pressure P_1 is greater than P_{cr}, it may be expected that the front structure will correspond to rapid compression from P_{cr} to P_0 and to a gradual continuous compression (because of viscosity) from P_{cr} to P_1. It may be mentioned that the effect of viscosity was detected neither in glycerol, which under

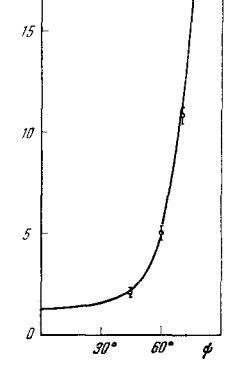

FIG. 3. Relationship between the reflection coefficient of the shock front in toluene and the angle of incidence. The solid line was calculated using Fresnel's equations for n = 1.95 (σ = 1.76), n_0 = 1.492. (○) = measured points [45].

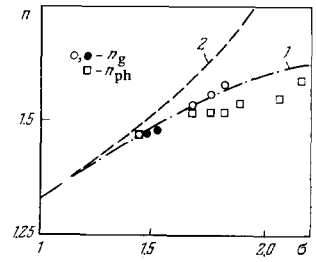

FIG. 4. Relationship between the refractive index of water and the degree of compression (σ) in the shock wave. 1 - calculated by the Lorenz-Lorentz formula (6); ○,□ = experimental points taken from [42]; ○ = experimental points taken from [59].

normal conditions has a much higher viscosity than water, nor in shock-compressed lucite and ionic crystals, which remain solid behind the shock front. In this respect the behavior of water is anomalous.

Studies of the reflectivity of the shock-wave front in condensed materials indicate also a very high smoothness (specular character) of the surface. This is shown qualitatively by the sharp definition of the edge in beams reflected from the shock front and by the absence of diffusion background (see for example Fig. 1,c).

A quantitative evaluation of the roughness of the shock front can be obtained on the basis of[47], where the effect of this roughness on front reflectivity was considered within the framework of the wave theory of light reflection.

When the front surface roughness is of the same order as the wavelength of the incident light λ, the intensity of specular reflection is reduced and diffuse reflection makes an appearance. If the surface irregularities have a random distribution[47], then

$$I_{rough} \approx I_{spec.} \exp(-4k^2 \overline{\Delta z^2} \cos^2 \psi), \qquad (4)$$

where I_{rough} and $I_{spec.}$ are the reflection intensities from rough and specular surfaces, $k = 2\pi/\lambda$, ψ is the angle of incidence, and $(\overline{\Delta z^2})^{1/2}$ is the degree of roughness. The nature of the light reflection and its intensity vary as functions of the degree of roughness (Fig. 5).

Since measured reflectivities agree, within the accuracy limits of the method, with values calculated from the refractive index measured under the same conditions (Fig. 2), it is reasonable to assume that the degree of roughness of the shock front does not exceed $(\overline{\Delta z^2})^{1/2} = 2 \times 10^{-6}$ cm.

In view of its high sensitivity to the roughness of the shock front, the light reflection method has beem employed[46,47,65,66]—as suggested by Zel'dovich—in the investigations of shock-wave smoothness in detonating liquid explosives. Considerable interest in this problem has arisen in recent years because of the work of Shchelkin[67,68], who suggested that, not only in gases but in condensed explosives as well, the one-dimen-

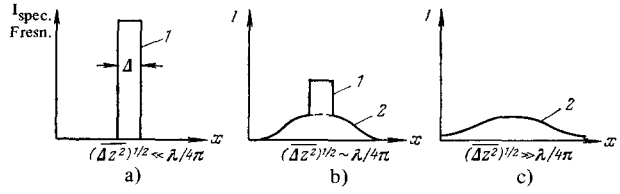

FIG. 5. Variation of the nature and intensity of light reflection (at specular reflection angle) as a function of the degree of surface roughness[47]. 1,2 – specular and diffuse reflections; Δ – width of light source.

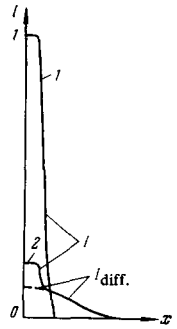

FIG. 6. Relative distribution of the intensity of light reflected from the detonation shock front [47]. 1,2 – overcompressed and normal detonations of the stoichiometric composition of dichloroethane and nitric acid.

sional state of the detonation wave is unstable [69]. The earlier work [46,47] dealt with an experimental investigation of the transparent explosive mixture of concentrated nitric acid and dichloroethane. The stoichiometric composition of this mixture (60/40 weight ratio) and its explosive properties are similar to those of TNT. Analysis of the results by the methods of wave theory of light reflection led to the conclusion [47] that the shock front in an exploding liquid is not perfectly specular. The front irregularities cause a lowered intensity of specular reflection and the occurrence of diffuse reflection. Figure 6 shows the intensity distribution of the reflected beam over its cross-section for various conditions; it can be seen that a reflection such as in Fig. 5a takes place in the case of normal detonation of the stoichiometric composition. In normal explosion, the roughness of the shock front does not exceed 10^{-5} cm, with a mean period of 5×10^{-4} cm. The average inclination angle of the irregularities is 1° [47]. The reason for the roughness of the front surface is still unclear [74]. We may have here a phenomenon similar to that observed in gas explosion [70], where the minimum scale in a mixture of $C_2H_2 + 2.5\ O_2$ was 10^{-2} cm, or else inhomogeneities may form in the zone of the chemical reaction and give rise to irregularities of the shock front (because of the subsonic velocity in the region between the wave and the reaction zone). However, this irregularity of the front has no noticeable back-effect on the reaction.

3. Density Dependence of the Refractive Index of Liquid Dielectrics. Anomalous Behavior of Shock-compressed compressed Carbon Tetrachloride.

In most of the publications on the dependence of the refractive index n of liquid dielectrics on the density ρ the results refer only to a relatively narrow range of densities, determined by their thermal expansion [71,72]. A somewhat wider range of densities was investigated in static compression [73-75]. The first of these papers [73] deals with the dependence of the refractive index of water, alcohol, and their mixtures in the pressure range extending to 1500 atm. In most cases, the experimental results can be described better [73,74,76] by the Gladstone-Dale empirical formula

$$\frac{n-1}{\rho} = \text{const}, \tag{5}$$

than by the Lorenz-Lorentz formula

$$\frac{n^2-1}{n^2+2} = \text{const} \tag{6}$$

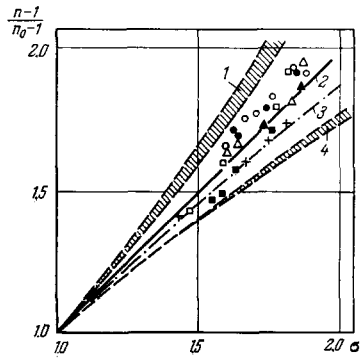

FIG. 7. Relationship between the refractive index of liquid dielectrics and the degree of compression [42,45]: ○ - toluene, $n_0 = 1.492$; ● – benzene, $n_0 = 1.496$; ▲ – acetone, $n_0 = 1.359$; ■ – glycerol, $n_0 = 1.472$; + – water, $n_0 = 1.333$; Δ – CCl_4, $n_0 = 1.457$; □ – ethanol, $n_0 = 1.362$. Method of calculation: 1 – (6); 2 – (5); 3 – (8); and 4 – (7).

or by Drude's equation

$$\frac{n^2-1}{\rho} = \text{const}. \tag{7}$$

The study of optical properties of shock-compressed matter enables us to determine $n(\rho)$ in a substantially greater range of densities exceeding the initial density by a factor of 1.5–2. These investigations were carried out [42,45,59] on several liquids. The results obtained by the photometric [45] and geometric [42,45,59] methods (see Sec. 1) are shown in Fig. 7. In the photometric method the refractive index was calculated from the measured reflection coefficients by means of Fresnel's formula. The degree of compression was found from the measured velocity of the shock wave and the already known [77] shock adiabats of the investigated liquids. It can be seen from Fig. 7 that the experimental data for various liquids are grouped around the straight line $(n-1)/(n_0-1) = \sigma = \rho/\rho_0$ [where n_0 and ρ_0 are the refractive index and the density at atmospheric pressure] which reflects the Gladstone-Dale dependence of refractive index on density. The experimental data never fall into the hatched areas whose boundaries delimit the Lorenz-Lorentz or Drude dependence $n(\sigma)$ for $n_0 = 1.33$ and 1.50. The correspondence of the measured data [71-76] and relations (5), (6) and (7) for $\sigma \approx 1$ is similar (Fig. 8).

Returning to Fig. 7, we note that, while the general agreement between the measured data and Eq. (5) is quite satisfactory, the data for toluene and benzene slightly deviate toward greater values of n, and those for glycerol and water are on the low side. It may be recalled that the temperature dependence of the refractive index was not taken into account in the above discussion. However, the measurements were carried out under such conditions that the dynamic application of pressure caused a rise not only of density but also of temperature. Thus, when water is shock-compressed

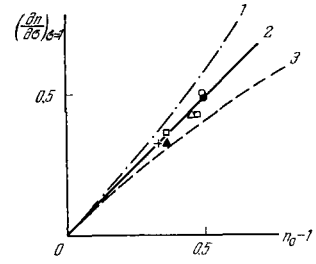

FIG. 8. Comparison of experimental values of $(dn/d\sigma)_{\sigma \approx 1}$ and values calculated from Eqs. (6) – 1, (5) – 2, and (7) – 3. Point designation as in Fig. 7.

by a pressure of 1440 atmospheres, its density rises to 1.75 g/cm^3 and its temperature to 875° C.[78] In[42] it was suggested that the combined effect of density and temperature on the refractive index of water can be described by the following equation:

$$n = 1.334 + 0.334(\sigma - 1) - 1.90 \cdot 10^{-5} T\sigma \qquad (8)$$

(where T is in °C and $\sigma = \rho/\rho_0$); the above expression gives in a satisfactory manner the refractive index of water vapor (which, according to experiments is $n = 1 + 0.33\rho$)[79] and that of ice[79] ($n = 1.311$ with $\rho = 0.9168$). The difference between (8) and the Gladstone-Dale formula is that the former contains a temperature term. In the range of densities and temperatures prevailing at the shock front in water, calculations by (8) (curve 3 in Fig. 7) yield satisfactory agreement with the measured values of the refractive index. The value of $(\partial n/\partial T)\rho$ in (8) was taken from[76]. The values of $(\partial n/\partial T)\rho$ for other liquids are of the same order.[76,74]

In[75] an effort was made to describe liquids by a modified Drude formula which took into account the change in the fundamental absorption frequency with change of density. The authors of[80] took into account the change in polarizability on compression in order to reconcile the analytical relations with the measurements. We shall discuss this problem in greater detail in the next section.

Let us look more closely at the results of the investigation of CCl_4, shown in Fig. 9. The ordinates are the measured reflectivities (normalized to $\psi = 30°$) at the fronts of shock waves of various intensities. It is evident that up to $\sigma \approx 1.9$ the reflection coefficients are no more than 2 or 3%, which shows satisfactory agreement with the Gladstone-Dale formula (several values are also found for other liquids, as shown in Fig. 7). As the intensity of the shock wave and the degree of compression increase, the function $R(\sigma)$ moves sharply upward, and at $\sigma \approx 2.15$ the measured reflection coefficient exceeds the value calculated from (5) by a factor of nearly 5. The $R(\psi)$ relation for CCl_4 is also anomalous when $\sigma = 1.95$. In all other investigated liquids $R(\psi)$ follows the Fresnel equations, but Fig. 10 shows that in the case of CCl_4 the light reflection from the shock front is considerably greater than would be indicated by the refractive index calculated from (5); moreover, with increasing ψ the fraction of reflected light increases faster than Fresnel equations indicate. Temperature measurements have shown (see Sec. 9) that the function $R(\sigma)$ for CCl_4 is similar to those for other liquids, provided the CCl_4 remains solid behind the shock front. The anomaly appears when $P \geq 300$ kbar and $T \geq 3500°$, when the originally liquid carbon tetrachloride remains liquid behind the shock front as well. The reason for this anomalous behavior of CCl_4 is still far from clear. It was suggested that this might be caused by a red shift of the edge of the fundamental absorption band, but investigations of the shock wave front reflectivity with incident wavelengths $\lambda = 4000$ Å and 2600 Å revealed no noticeable differences in the reflection coefficients, i.e., they showed the absence of dispersion. Measurements of the conductivity and absorption power in shock-compressed CCl_4 may establish[30] whether the discussed effect is not due to a high concentration of free electrons[45]. This is perhaps to some extent indicated by the results presented in Fig. 10.

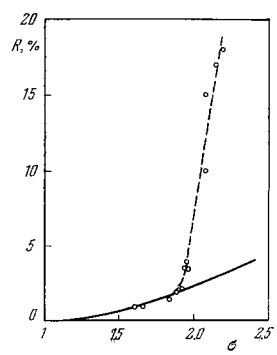

FIG. 9. Reflectivity of the shock front in carbon tetrachloride as a function of the degree of compression [45]. O (– – –) measured data; the solid line represents values calculated by (5).

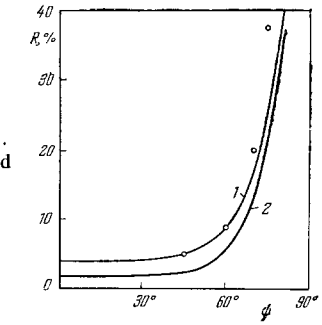

FIG. 10. Reflectivity of the shock front in carbon tetrachloride as a function of the incidence angle, for a degree of compression $\sigma = 1.95$. O – measured, —— graphs calculated by Fresnel's equations for n_{21}: 1 – corresponding to the experimental point at $\varphi = 45°$, 2 – calculated by (5) for $\sigma = 1.95$.

4. Investigation of the Optical Properties of Shock-compressed Ionic Crystals. Nonequilibrium States.

The methods described in Sec. 1 have been used to investigate the optical properties of some shock-compressed alkali halides[43]. The results for single crystals of LiF, NaCl, and CsBr, none of which undergoes polymorphic transformation in the employed pressure range, are shown in Fig. 11. In the case of NaCl, CsBr, KCl and KBr, which cease to be transparent, the reflection coefficient at the shock front was measured, and the refractive index was calculated assuming Fresnel's equations to be valid. In the case of LiF, which remains sufficiently transparent up to 700 kbar at least, the refractive index in the compressed state was found directly from the course of the beam, using the geometric method (cf. Sec. 1). The degrees of compression were obtained in[16,17,49]. Figure 11 shows that the relationship between the refractive index and density may be written as

$$n(\sigma) = n_0 + \frac{dn}{d\sigma}(\sigma - 1) \qquad (9)$$

where $dn/d\sigma$ is a constant with a different value for

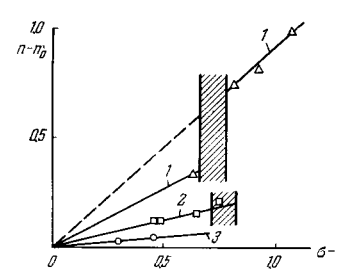

FIG. 11. Dependence of the refractive index of ionic crystals on the degree of compression σ[43]. Δ,□, O – measurements on: 1 – CsBr, 2 – NaCl, 3 – LiF. The melting regions of CsBr and NaCl are hatched.

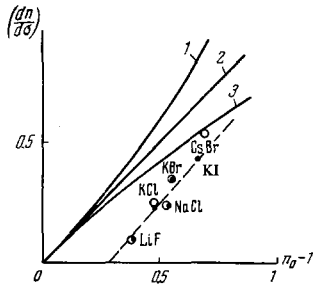

FIG. 12. Comparison of measured values of $(dn/d\sigma)_{\sigma=1}$ with those calculated by Eqs. (6) – 1, (5') – 2, and (7) – 3: ○ – measurements acc. to [43]; ● – measurements at $\sigma \approx 1$ (after [81-83,85]); – – interpolation of measurements.

each crystal. In contrast to liquids, we have here $dn/d\sigma < n_0 - 1$.

We shall first consider the values of $n(\sigma)$ measured in the solid phase. In all investigated crystals $dn/d\sigma$ has been found to be substantially smaller than could be expected on the basis of the Lorenz-Lorentz, Gladstone-Dale, and Drude formulas (Figure 12). A similar difference in the initial slope of the function $n(\sigma)$ was found earlier[81-83] from investigations of the photoelastic characteristics of ionic crystals (cf. Fig. 12 and the fourth and fifth lines in Table I). Direct measurements of the refractive index in NaCl, KBr and LiF under hydrostatic compression, with pressures up to 1 kbar[80], produced, for the first two crystals, results close to those mentioned earlier (see the sixth line in Table I). In the case of LiF, Waxler and Weir[80] did not record any change in n, and concluded that at high compressions the refractive index n in LiF and in other crystals should decrease. This conclusion contradicts the above-quoted results of measurements carried out on shock-compressed ionic crystals. It also contradicts the results of[84], where it was established that the refractive index of LiF increases linearly in the entire investigated pressure range up to 7 kbar; the value of $\rho_0 dn/d\rho = dn/d\sigma = 0.132$ given in[84] is close (see Table I) to the results of studies of the photoelastic characteristics[81-83] and to results obtained in shock-compression[43].

We now turn to another interesting property of $n(\sigma)$, revealed in[43]. The experimental study of $n(\sigma)$ in the shock-compression of ionic crystals covers also the range of densities in which the ionic crystals at the shock front become liquid because of heating. The problem of melting in shock compression will be discussed in detail in Sec. 8. For the moment we shall only say that both the refractive index and its derivative increase sharply during melting in the compressed state. Thus, in the case of CsBr, melting causes the refractive index to increase (Fig. 11) from 2.05 to about 2.45. The experimental results obtained for the liquid phase of shock-compressed crystals of CsBr, KCl, and KBr are satisfactorily described by the same equation (9) as are those for the solid state, but $dn/d\sigma$ is about 1.5–1.7 times larger (cf. Table I). It has been shown[43] that at atmospheric pressure the change in the density of liquid alkali halides causes a change in the refractive index about 1.5 times as large as that in the solid state. Figures 11 and 12 and Table I indicate that, in a wide density range, $n(\sigma)$ for each of the phases, solid and liquid, can be separately described (though only approximately) by expressions similar to (9), with $(dn/d\sigma)_{liq} > (dn/d\sigma)_{sol}$, having a common point at $\sigma \approx 1$, as shown qualitatively in Fig. 13. This may explain the apparent contradiction whereby at atmospheric pressure melting brings about a lowering of the refractive index, while in the compressed state melting increases it (cf. Fig. 13).

Let us consider briefly the physical nature of the above effects. The refractive index is known to increase with increasing density and electronic polarizability, and the latter determines almost wholly the dielectric constant in the region of optical frequencies. Since the refractive index of alkali halides increases more slowly with density than would be expected from the Lorenz-Lorentz or Drude equations, it apparently follows that, as the interionic spacings are reduced, the deformability of the electron shells of ions acted upon by light is reduced because of the increased repulsion forces. In other words, compression causes a decrease in the electronic polarizability of the ions. This was first pointed out by Muller[81]. According to Burstein and Smith[82], the decreased polarizability of ionic crystals accompanying the reduction in interionic spacing is due to an overlapping of the electron shells, i.e., to an increased ratio of covalent to ionic bonding. In crystals such as MgO, diamond, etc. which have a high degree of covalent bonding, the refractive index, according to those authors, actually decreases as the density is increased. An analogous effect has been discovered in ZnS and Al_2O_3.[85] In all these cases decreased electronic polarizability not only compensates but even predominates over the effect of increasing density. An increase in the part played by covalent bonds when ionic crystals are compressed seems quite likely, since the rising density is associated with a rise in repulsion forces, which are determined by exchange and overlap of electron shells.

Table I

	Crystal	LiF	KCl	NaCl	KBr	KI	CsBr
	n_0	1.392	1.490	1.544	1.559	1.667	1.698
Solid Phase	Compression range σ [43]	1.30–1.48	1.68	1.45–1.68	1.70	—	1.63
	$\frac{dn}{d\sigma}$ [43]	0.1	0.25	0.24	0.35	—	0.54
	$\left(\frac{dn}{d\sigma}\right)_{\sigma\approx1}$ [81–83]	0.1	0.23	0.24	0.35	0.43	0.48
	$\left(\frac{dn}{d\sigma}\right)_{\sigma\approx1}$ [80]	0.0	—	0.28	0.35	—	—
	$\left(\frac{dn}{dT}\right)_{\rho}\cdot10^5$ [177]	0.26	−1.04	−0.78	0.0	—	—
Liquid phase	Compression range σ [43]	—	1.83–1.98	—	1.88	—	1.8–2.07
	$\frac{dn}{d\sigma}$ [43]	—	0.35	—	0.53	—	0.9

FIG. 13. The character of the dependence of the refractive index on density (degree of compression) in the solid (1) and liquid (2) phases of ionic crystals. The numerical values are those for CsBr. A – melting region at atmospheric pressure, B – melting region in a shock-compression state.

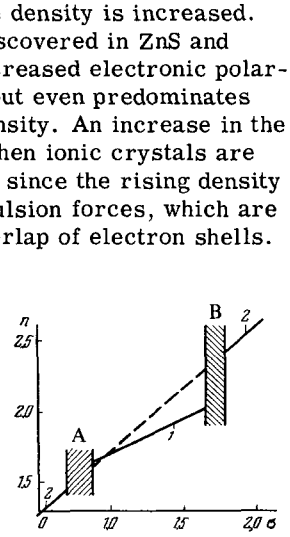

The fact that overlap forces are not taken into account is one of the reasons that the Lorenz-Lorentz formula is unsatisfactory for describing the $n(\sigma)$ dependence; the above formula is derived assuming that there is no "overlap" between ions. On the basis of all these qualitative considerations, the difference between the values of $dn/d\sigma$ in the solid and liquid phases of ionic crystals may be connected with the change in the nature of bonds occurring when the crystals are liquified[43]. It is also well known that the change of aggregate state without any changes in the nature of the bonds has little effect on the polarizability of atoms or ions[86]. The above considerations are only qualitative. For the purpose of quantitative discussion, Muller introduced a correction factor that allows for the change of ion polarizability on compression:

$$\left(\frac{dn}{d\sigma}\right)_{expt} = \left(\frac{dn}{d\sigma}\right)_{calc} (1-\lambda_0), \qquad (10)$$

where $(dn/d\sigma)_{calc}$ is taken from Lorenz-Lorentz or Drude equations and λ_0 expresses the degree of covalence of the bonds. Expression (10) is widely used[80-83,87] in discussions of experimental data and for their analysis. The difference in the value of λ_0, depending on the starting analytical formulae, indicates that the parameter λ_0 is purely empirical. Moreover, for liquids $\lambda_0 > 0$ if the Lorenz-Lorentz equation is employed for $n(\sigma)$, and $\lambda_0 < 0$ if the Drude formula is used. The difficulties in determining the internal fields in crystals, even in the case of alkali halides, make it impossible at present to calculate theoretically their dielectric constants. The work of Yamashita and Kurosawa is, however, a step in this direction[88,89].

Let us now consider the results of an investigation of the reflectivity of the shock front in KCl and KBr.[43] The results for KBr are illustrated in Fig. 14, and it can be seen that, when $\sigma = 1.7-1.9$, the measured points can be described by a relation such as (9) with $dn/d\sigma$ following from the studies[81-83] of the photoelastic characteristics, as with other crystals (see above). There is a noticeable deviation from this relationship in the case of KBr at $\sigma = 1.54$ and in the case of KCl at $\sigma = 1.52$. The reflection coefficient is here 2–3 times smaller than would be expected. In[43] this difference was attributed to the fact that at pressures lower than ~ 150 kbar the polymorphic transformation of KCl and KBr into the CsCl structure[15] takes place within a time $\tau > 10^{-12}$ sec. In this case the incident light is reflected from a layer of substance that remains in metastable state at the shock front (point 1 in Fig. 15), which corresponds to the dynamic adiabat of the first phase of the substance. Since this is steeper than the adiabat of the second phase, a smaller refractive index (point a in Fig. 14) corresponds to the smaller density jump at the shock front. The nonequilibrium states of the first phases of KCl and KBr[43] are given in Fig. 15 (points A). The same figure shows also the positions of the adiabats of the first phases of KCl and KBr, calculated by Urlin using the state equations developed in[49]. When the pressure is higher, the temperature rises, the relaxation time is reduced, and the phase transformation occurs in a layer very much thinner than $\lambda/2\pi$. In this case, the refractive index corresponds to the total volume jump behind the shock front (point 2′ in Fig. 15), and this has been confirmed experimentally (Fig. 14). Hence, the polymorphic transformation in KCl and KBr during shock compression with a pressure of $P = 200-210$ kbar takes place in less than 2×10^{-12} sec. The melting process at the shock front occurs within the same time, although in the case of KBr, in contrast to CsBr (Figs. 14 and 11), melting in the narrow near-frontal layer occurs also at higher pressures than behind the shock front.

5. Optical Study of Elastoplastic Waves in Glass

In[44] the method based on light reflection was applied to an investigation of elastoplastic flow in TF-5 lead glass (heavy flint). The transition from elastic to plastic state under shock conditions was first investigated in a number of metals[90-98]. Transition to plastic flow condition has also been recorded for materials as brittle as quartz[99], copper glass[100] and silicon[1]. Figure 16 shows schematically the form of the Hugoniot adiabat for this case. Up to the pressure P_1, determined by the dynamic yield point, the material is compressed elastically. The nonequilibrium elastic adiabat, part of which is the section 0-1, is shown in Fig. 16 as a dot-dash line. In the pressure range between P_3 and P_1 two waves travel in the material (Fig. 16, b): an elastic wave with velocity c_{el}, and a plastic wave with velocity $D_2 = u_1 + D_{21}$, where u_1 is the velocity of the material behind the front of the elastic wave and D_{21} is the velocity of the wave with respect to the material ahead of its front. With increasing pressure the plastic wave veloc-

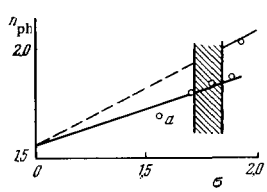

FIG. 14. Refractive index of KBr as a function of the degree of compression. O – measured points [43]; the melting region of KBr under shock-compression is shown hatched; a – point corresponding to the metastable state at the shock front.

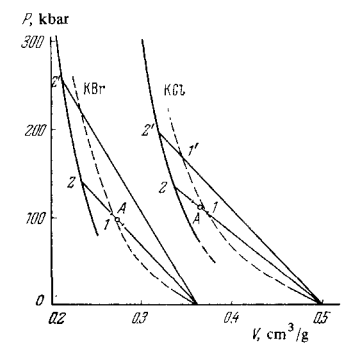

FIG. 15. Equilibrium (——) and non-equilibrium (– –) adiabats of KCl and Kbr [1,49,43]. O – experimentally detected states on nonequilibrium adiabats [43]; 1(1′), 2(2′) – states on non-equilibrium and equilibrium adiabats, respectively.

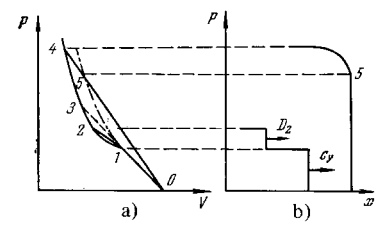

FIG. 16. P-V diagram for lead glass (a) and structure of shock waves in elastoplastic flow (b).

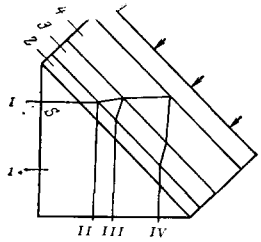

a)

b)

FIG. 17. Diagram of the experiment (a) and photochronogram (b) in the investigation of the reflectivity of the shock front in lead glass: 1 – prism; 2 – liquid (CCl_4); 3, 5 – glass; 4 – liquid. Oa, ab – reflection from the shock front; a' a, b' b – reflection from the glass/liquid boundary.

FIG. 19. Photographic record of an investigation of the reflectivity of the shock front induced by the impact of a thin metal plate on lead glass: t_1 – the instant when the rarefaction wave catches up with the shock wave; t_2 – the instant when the shock wave splits into elastic and plastic waves; cc' – "pause" associated with the difference in arrival times of the plastic and elastic waves at the glass boundary.

ity increases, while the velocity of the elastic wave that carries the critical yield-point pressures, remains unchanged. When the pressures become greater than P_3, the elastic and plastic compression zones come closer together and form a unified profile of the shock wave (Fig. 16,b).

This pattern is clearly demonstrated when the reflectivity of the shock front is investigated in experiments carried out as shown in Fig. 17. Investigations[44] have shown that $P_1 = 79$ kbar in lead glass. At pressures $P_1 < P < P_3 = 170$ kbar we find in lead glass a constant velocity $\bar{c}_{el} = 3.77$ km/sec ($t_b - t_{c'} = \text{const}$), independently of the applied pressure. This velocity agrees quite satisfactorily with the value $c_{el} = 3.67$ km/sec calculated from Young's modulus E, Poisson's coefficient μ, and density of lead glass ρ_0 by means of the following formula:

$$c_{el} = \sqrt{\frac{E(1-\mu)}{\rho_0(1+\mu)(1-2\mu)}}.$$

When the pressure P is less than 170 kbar, the boundary between the lead glass and the liquid is reached first by the elastic and then by the plastic wave. Because of their different instants of arrival, there is a "pause" of corresponding duration. When P approaches the value of P_3, D_{21} increases and the duration of the pause is reduced. The weak reflection, which fails to be detected in the experiment with a two-wave configuration propagating in lead glass, is due to the fact that density jumps (and consequently the jumps of the refractive index) for each of the two waves are relatively small. Whereas one wave with an amplitude of 170 kbar reflects about 0.5% of the incident light, upon stepwise loading to the same pressure the elastic and plastic waves reflect only 0.1–0.15%. When the pressure becomes greater than P_3, the regions of elastic and plastic compressions come together and form a unified profile of the shock wave. The velocity of this wave is greater than c_{el}; the "pause" disappears, the shock wave front reflects the incident light, and the reflectivity increases with increasing pressure (Fig. 18). When $P > 265$ kbar ($\sigma > 1.46$), this rise takes place in accordance with the density jump at the front, and in the region of $P < 265$ kbar the measured reflection coefficients are smaller than calculated ones. This is caused by the relaxational character of the transition to the plastic state. The material is first elastically compressed to the state of point 5 of Fig. 16, and the reflection corresponds to the density jump along a nonequilibrium elastic compression adiabat. At $P > 265$ kbar the time of transition into the plastic state is $\tau \leq 10^{-12}$ sec. At the front of a shock wave having a sharp profile, the density jumps from its initial to the ultimate value. This is because the function $n(\sigma)$ becomes linear starting with such pressures, as was also observed in ionic crystals not undergoing polymorphic transformations. The results shown in Fig. 18 were obtained using various shock intensities in glass. The solid line in Fig. 18 was obtained in an experiment (Fig. 19) with a setup somewhat differing from that of Figure 17,a. It was mentioned earlier that at $P < 170$ kbar lead glass remains partly transparent (see Figure 17,b), whereas at $P > 170$ kbar it becomes almost completely opaque. This difference in the behavior of glass is apparently due to the difference in the nature of its compression. The loss of transparency is evidently caused by disturbance of the optical homogeneity of the plastically deformed glass, whereas in elastoplastic compression this process is not fully realized.

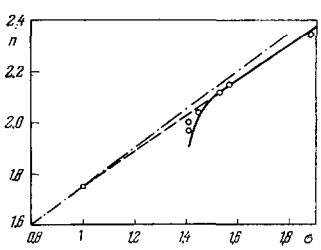

FIG. 18. Refractive index of lead glass as a function of the degree of compression [44]: ○ – experimental data obtained by the photometric method; □ – n_0; –.– n (σ) in accordance with (9) with $dn/d\sigma = n_0 - 1$; – – interpolated function $n(\sigma)$.

6. Phase Transition of Water into Ice VII Under Shock Compression

Phase transitions of water into various crystalline types of ice under high pressures were first discovered by Bridgman[101] in the investigation of the isothermal compressibility of water up to $P \approx 40$ kbar. The phase equilibrium line for ice VII and water was later inves-

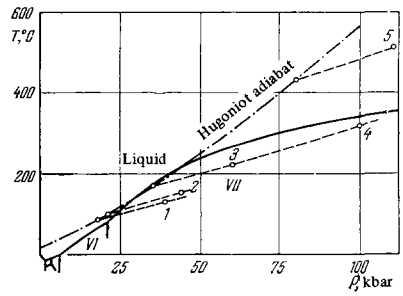

FIG. 20. Phase diagram of water: — phase boundaries [101,102]; —·— Hugoniot adiabat [78]; – – compression by the second shock wave; O – experimentally investigated states.

tigated by Pistorious et al.[102] up to 200 kbar. The phase diagram of water constructed from these results is shown in Fig. 20, which also gives the Hugoniot adiabat of water from the data of Rice and Walsh[78]. The temperatures of shock-compressed water calculated by Rice and Walsh were checked experimentally by Sinitsyn, Kuryapin and the present writer[49] using the method of the photoelectric pyrometry. The experimentally found temperatures for P = 300—400 kbar (Fig. 21) are sufficiently close to the calculated values, and are smaller than the latter by about 10%. This means that we can use the data of Rice and Walsh[78] for necessary estimates in a wide range of pressures. It follows from the phase diagram that the dynamic adiabat runs in the liquid state over nearly the entire considered pressure range, and only at pressures between 30 and 45 kbar does it encroach on the region in which water and ice VII coexist. The values are only approximate, since the Hugoniot adiabat of water in Fig. 20 does not take into account its entrance into the two-phase region. Walsh and Rich[77] investigated the transparency of water in the pressure range between 30 and 100 kbar by photographing a coordinate grid illuminated by an external source of light through shock-compressed water (Fig. 22). The quality of the photographs was taken as the measure of the transparency. The authors did not find any absence of transparency of the water in the entire investigated range of pressures. Al'tshuler et al.[103] reached a different conclusion; having investigated the dynamic adiabatic of water up to 800 kbar, they found a density jump at 115 kbar and identified it with a phase transition of water. This conclusion was also reached as a result of investigations of the transparency of water under shock compression, using a method similar to that of Walsh and Rice. The range of pressures investigated for this purpose was extended in[42] to 300 kbar, and no loss of the light intensity was detected between 40 and 300 kbar when light passed twice through the compressed water. This confirms the conclusion that the water remains liquid along the shock adiabat. At the same time, calculations show that it is possible to enter the region of existence of ice VII, or at least the two-phase region, when the pressure is applied in steps, provided the first wave carries pressures of 20—40 kbar. Compression of matter by a few successive shock waves can be realized[176] by using screens of alternating layers of different dynamic rigidities. A shock wave passing through such a layer splits into a series of waves chasing one another. The material for these layers was chosen such as to control the wave intensity; and their thickness was such that the second shock wave caught up with the first one within the investigated layer of water. One of the obtained photochronograms and the diagram of the setup are shown in Fig. 23. The following processes can be distinguished in the photochronogram (Figs. 23 a,b). At the instant 0 the shock wave enters the water. At the instant 3 the second shock wave catches up with the first one. After this the wave becomes stronger, as evidenced by the increase in its reflectivity (ray 0-1) and by the kink due to the increased velocity. The ray 0-2 corresponds to light reflection from the piston. At the instant 2, the layer of compressed water becomes opaque, and the light reflection from the piston is no longer recorded. Finally, at the instant 4 there is a considerable fogging of the photochronogram, which indicates diffusion scattering of the incident light. The loss of transparency and occurrence of diffusion scattering of the light can be attributed[176] to the formation of a finely crystalline phase of ice VII having a refractive index differing from

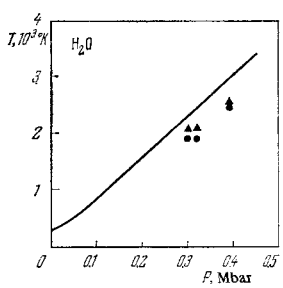

FIG. 21. Temperature of water behind the shock front as a function of the front pressure: ▲,● measurement with λ = 0.478 and 0.625 μ; — calculated [78].

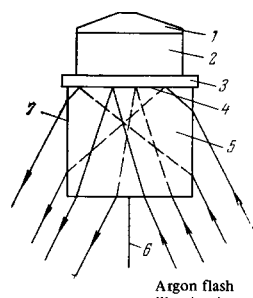

FIG. 22. Layout for the investigation of transparency of shock-compressed water[77]. 1 – generator of a plane detonation wave; 2 – explosive charge; 3 – metal plate; 4 – coordinate grid; 5 – water; 6 – plate delineating the light beam; 7 – vessel with transparent walls.

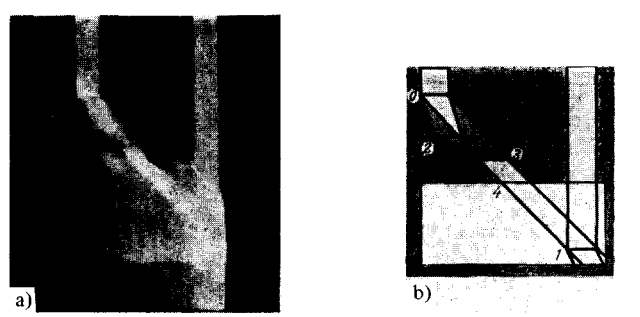

FIG. 23. Photographic record (a) [and its scheme (b)] of the phase transformation of water into ice VII during compression with two shock waves: 0 – entrance of the shock wave into water; 3 – shock wave overtakes the first wave; 2 – water loses transparency; 4 – onset of diffuse scattering.

that of compressed water. When the experimental conditions are suitably varied, it is possible to obtain such states (points 1-4 in Fig. 20) over a fairly wide range of pressures. When the pressure of the first shock wave is increased, states known to correspond to the liquid phase are realized behind the second wave (point 5 in Fig. 20). All these results show convincingly that in spite of a certain relaxational character of the process[176], under certain conditions water manages to freeze behind the front of the shock wave in a time of the order of 10^{-6}—10^{-7} sec. We shall discuss in Sec. 9 another case in which a liquid (CCl_4) solidifies under shock compression. Van Thiel and Alder have reported[104,105] that, according to their results, liquid argon passes into a region of coexistence of solid and liquid phases under shock compression, i.e. that it freezes partly.

II. EQUILIBRIUM RADIATION OF THE SHOCK-WAVE FRONT. EXPERIMENTAL DETERMINATION OF TEMPERATURES.

7. Possibility of Temperature Measurement in Shock-compressed Condensed Materials. Principle of the Method

The requirements of aviation, rocket engineering, and other branches of modern technology, as well as the relative simplicity of the generation and measurement of shock waves in gases, have resulted in a great number of published reports dealing with these subjects both in the Soviet Union and abroad. Reviews of work on the shock compression of gases (including the temperature measurement), listing the original literature, will be found in[2] and[106-109]. The highest temperatures in shock-compressed air and inert gases were achieved by Model'[110-111], and in argon by Roth[112]. Both authors used explosives to generate the powerful shock waves. Several papers are devoted to the measurement of temperature and investigation of the spectral distribution of the radiation from the detonation front in condensed explosives[113-118].

Since shock-wave experiments involving explosions in condensed matter are laborious and quite complex, the number of such investigations is very much smaller than of those dealing with gases. This is particularly true of the temperature measurement in shock-compressed bodies. It is possible that a certain part was also played here by the contradictory attitude of some American workers (see for instance the papers by Alder[20] and Deal[54]. For this reason, up to very recent times the investigations of the thermodynamic properties of condensed materials at the high pressures created by shock waves were limited to measuring the kinematic parameters of the shock wave, i.e., its velocity D and the mass velocity u of the matter behind the wave front. With the aid of the conservation laws, the above parameters make it possible to find the pressure P, density ρ, and increase in internal energy E.[5,6] The temperature T, which is one of the fundamental thermodynamic characteristics of the state of matter, was found analytically by using various assumed equations of state[5-17].

Direct measurement of temperatures of shock-compressed condensed bodies provides an opportunity for checking and broadening the existing ideas about the equation of state and the properties of matter at high pressures. Such studies were initiated by the present writer in 1956, together with Sinitsyn, Kirillov, and Kuryapin. Let us consider some basic problems of these measurements. Since the matter remains in the shock-compressed state for a very short time, and the temperatures are very high, of the order of thousands or even tens of thousands of degrees, the best methods for the temperature measurements are provided by the optical approach[119,110,120,121] based on the relation between the radiation of a body and its temperature. However, many solids are not transparent, and this is the difficulty when optical methods are to be employed for determining the temperature of a material when the shock wave propagates through it. In this case, information about the state of the material can be gathered only after its expansion[2,122,123]. Transparent substances, which make it possible to record the radiation of the layer not yet reached by the shock wave, are thus of special interest. The radiation of the investigated material characterizes its temperature if it is thermal radiation; the material and the radiation are in equilibrium. When the material is shock-compressed, the mechanical energy is first imparted to the lattice and only then to the electrons, whose energy is of interest to us, because the radiation is recorded in the visible part of the spectrum. Establishment of thermodynamic equilibrium is determined by the phonon-phonon and phonon-electron interactions. The time required for the establishment of the phonon-phonon equilibrium is equal to the phonon mean free path (about 10^{-7} cm) divided by the speed of sound (about 4×10^5 cm/sec), i.e., about 10^{-12}—10^{-13} sec. The time of an electron-phonon interaction is 10^{-13}—10^{-14} sec, and since the electron gains an energy $h\nu$ during each act of interaction, where ν is the lattice-vibration frequency, the equilibrium between electrons and the lattice is reached at $\Delta T \sim 1$ eV in 10^{-11}—10^{-12} sec. It is also necessary to allow for the time required for thermal excitation of the electrons into the conduction band. Analysis of this process shows that the equilibrium temperature between the electrons and the lattice is established behind the shock front in about 10^{-9} sec (for further details see Sec. 13), i.e., within a thickness of about 10^{-3}—10^{-4} cm. This layer will not screen the equilibrium radiation of the compressed material if the absorption coefficient α is below 10^3 cm^{-1}. As will be shown in Sec. 10, in shock-compressed ionic crystals $\alpha \leq 10^2$ cm^{-1} when $T \leq 1$ eV. In this case the front of the shock wave emits equilibrium radiation which can be employed for the temperature measurement. It has been estimated that radiation losses at $T \leq 4$ eV are no more than 0.1%, and, of course, they can be neglected. Consider yet another aspect of the problem. It has been established both theoretically[124,2] and experimentally[110,111] that when strong shock waves cause luminescence in gases the brightness temperature of the wave front is substantially lower than the calculated value. The reason is that, when $T > 1$ eV, the gas in advance of the front is heated by radiation emanating from the front, becomes opaque, and screens the "hotter" front of the shock wave. In shock-compressed condensed materials this effect does not play any part. Indeed, the change of temperature ΔT_h in the

layer in advance of the wave front, caused by the radiation heating, can be evaluated from the condition that in the stationary case the radiant flux is equal to the flux of the material energy ahead of the front*:

$$n^2\sigma T_f^4 = \rho c_v D\,\Delta T_h,$$

where n is the refractive index, σ is the Stefan-Boltzmann constant, D is the shock-wave velocity, ρ and T_f are the density and temperature behind the front, and c_V is the specific heat. If $T_f = 50 \times 10^3$ °K and $D = 10^6$ cm/sec, we have $\Delta T_h = 40 \times 10^3$ for air but only 20° C for NaCl. This enormous difference in the temperatures of gases and solids heated by the radiation can be ascribed almost wholly to the difference between their densities.

Of all optical methods, the brightness method is the most suitable for measuring high temperatures of bodies with a continuous radiation spectrum. Its accuracy is better[110] than that of, say, the color method, especially at high temperatures when the relative energy distribution in the visible part of the spectrum, from which the color temperature is found, becomes little sensitive to temperature variations. The continuity of the radiation spectrum emitted by the shock front in condensed substances was confirmed in[49] on an SFR high speed camera with a special spectrographic attachment.

The brightness method for measuring the true temperature is based on Planck's and Kirchhoff's laws. According to these, the true temperature T of a body is given by the following equations

$$\left[\exp\left(\frac{C_2}{\lambda T}\right) - 1\right]\left[\exp\left(\frac{C_2}{\lambda T_s}\right)\right]^{-1} = \frac{\varepsilon_s(\lambda, T)}{\varepsilon(\lambda, T)}\,a(\lambda, T), \qquad (11)$$

$$a(\lambda, T) = \frac{\varepsilon(\lambda, T)}{\varepsilon^0(\lambda, T)} = 1 - \tau - r. \qquad (12)$$

In these equations $C_2 = 1.438$ cm-deg is the radiation constant, λ is the wavelength, ϵ_S the spectral brightness of a standard source having a known brightness temperature T_S(°K), while $\epsilon(\lambda, T)$ and $\epsilon^0(\lambda, T)$ are the respective spectral brightnesses of the measured body and a black body.

The spectral degree of blackness $a(\lambda, T)$ may differ from unity both because of the transparency of the material behind the front of the shock wave τ and because of the reflectivity of the front r. Experiments have shown[49,30] (cf. Sec. 10) that the investigated condensed materials become opaque in considerably thinner layers than shock-compressed gases[110]. For this reason, we may either neglect transparency, beginning with a certain thickness of the compressed material, or introduce a correction that does not exceed 10% of the measured temperature[49]. For pressures of the order of 1 Mbar the experimentally-determined reflectivity of the shock front[42-45] (cf. Secs. 3 and 4) is so small ($r < 2\%$) that it can be neglected in the temperature measurements (CCl_4 is an exception; see Sec. 3). When the temperatures of shock-compressed materials are measured, the recorded optical effects last only about 10^{-6} sec, so that highly sensitive and fast-responsive apparatus must be used. The measurements are therefore carried out photographically[110,52] (using SFR-type cameras) or photoelectrically[123,112,49,30]. The radiation receivers are either photographic films or photomultipliers.

Under the actual conditions of a detonation experiment, the photoelectric method makes it possible to measure temperatures beginning from $T_{min} \sim 1500$°K,[49] which corresponds to a light flux about 10^5 times smaller than would be possible with a photographic method ($T_{min} \sim 4500$°K), and at the same time the separated spectral range is reduced by a factor of 3—5. If the photomultiplier is placed near the investigated body, the lower limit of the recordable temperature may be appreciably reduced[123]. Another advantage of the photoelectric method is the ease of processing the experimental data. On the other hand, the photographic method makes it possible to observe the brightness distribution over the investigated surface. The time resolution of both methods may reach 10^{-7} to 5×10^{-8} sec. Separation of sufficiently narrow spectral intervals in various parts of the spectrum is achieved by means of special glass ($\Delta\lambda \approx 500$ Å) or interference ($\Delta\lambda \approx 100$ Å) filters. An IFK xenon flash lamp may be employed[126,49] as the standard light source for the visible part of the spectrum; the lamp itself is calibrated against an SI-16 ribbon incandescent lamp, using the measuring apparatus. The experimental results are most suitably processed by the method of actinic fluxes[127] (see also[49]). Details of the experimental setup and the characteristics of the apparatus have been given earlier[110,49,30].

8. Measurement of Temperatures of Shock-compressed Ionic Crystals and Establishment of their Melting Curves for Pressures up to 0.5—3 Mbar

Alkali halides are a very suitable subject for temperature measurement under shock compression, since they are optically isotropic and their single crystals are transparent in the entire visible part of the spectrum. This makes it possible to view the radiation of the heated material in the shock wave through a layer that has not yet been compressed. The compressibility of this class of ionic crystals under dynamic loading has been investigated in sufficient detail[15-17,49,20,128].

The dependence of the temperature of NaCl, KCl, KBr, and CsBr on the shock-wave pressure is shown in the phase diagrams in Figs. 24—27. The results of the investigations on NaCl and KCl are given in[49]; KBr, CsBr, and LiF have been investigated by the same authors. The difference between the temperatures found by measurements in the blue ($\lambda = 0.478\ \mu$) and red ($\lambda = 0.625\ \mu$) regions of the spectrum does not signify absence of black-body radiation, and apparently is only a result of inaccuracy in measurements[49].

All the investigated crystals are characterized by the same form of the shock adiabat in temperature-pressure coordinates. When the pressure is relatively small, their growth is accompanied by rising temperature, after which the temperature remains nearly constant, and when the pressure is increased further the temperature begins to rise once more. The authors of[49] attributed the temperature plateau in the T(P) plot to the melting of the ionic crystals. In point of fact, the thermal energy transferred to the body increases continuously with increasing shock-wave pressure, and,

*For the necessity of introducing the factor n^2 into the Planck and the Stefan-Boltzmann formulae see [125].

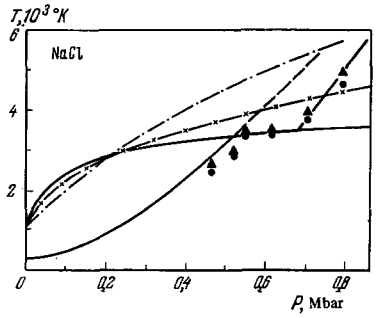

FIG. 24. NaCl phase diagram [49] (the melting curve at high pressures was determined in [49] from results of temperature measurements in shock-compressed material). ▲, ● – temperatures measured at $\lambda \approx 0.478$ and 0.625 μ. Dynamic adiabats: — calculated as in [49]; – – – same but with "superheated" solid phase. Melting curves: —— calculated as in [49]; – X – extrapolation of the data in [136] and [137] using Simon's equation; –·– calculated by means of the Lindemann–Gilvarry expression [134,135].

beginning at a certain pressure (2 in Fig. 28), the initially solid body should begin to go over into the liquid state. The further course of the function T(P) along the dynamic adiabat can be explained[49] by analogy to melting at atmospheric pressure, when an increase in energy supplied to the body that has started to melt does not cause any rise of temperature until the melting process has been completed. Further heating causes then once more a rise in temperature. The general pattern should be similar in the case of shock compression, with the difference that a certain temperature rise must be expected in the two-phase region (section 2–3 in Fig. 28), since $dT/dP > 0$ for the melting curves of most so-called normal substances. We shall estimate the possible temperature difference for the same pressures on the shock adiabatic, but with (3,4 in Fig. 28) and without account (point 5) of the melting process. The equilibrium condition for the two phases leads to[49]

$$T_5 - T_3 \approx T_3 \frac{\Delta S}{3Rn} = \frac{L}{3Rn}. \qquad (13)$$

The subscript 3 refers to the solid and 4 to the liquid phase on the melting curve; L is the heat of melting, and $\Delta S = S_4 - S_3$ is the entropy change during melting. It follows from (13) that, when melting is taken into account, the liquid-phase temperature (point 4) is lower than when melting is neglected (point 5); the temperature difference is approximately equal to the heat of melting divided by the specific heat of the material. In most simple substances and inorganic compounds the sharp rise of entropy on melting at atmospheric pressure is fairly constant and amounts to 1/3–1/2 of the specific heat of the material. We shall make use of this fact and assume[49] that, when a substance is compressed, its entropy jump will remain constant, independently of the applied pressure. Taking then, for example, $\Delta S/3Rn = 0.5$ and $T_3 = 4500°K$ for NaCl, we find that $T_5 - T_3 \approx 2200°K$. This figure is very close to the measured value (cf. Fig. 24). It follows from the above discussion that neglect of melting in a shock-compressed body leads to errors in the calculation of its thermodynamic parameters. On the other hand, direct measurement in a shock-compressed body is a very sensitive method for finding the melting curves, since the energy required for melting gives rise to sharp bends in the shock adiabat in the T-P plane. Urlin[129] reached the same conclusion after an analysis of the melting process in shock-compressed metals; in an earlier work[130] the same writer proved analytically that melting has little effect on the kinetic parameters

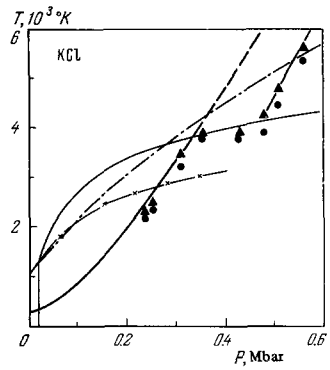

FIG. 25. Phase diagram of KCl [49].

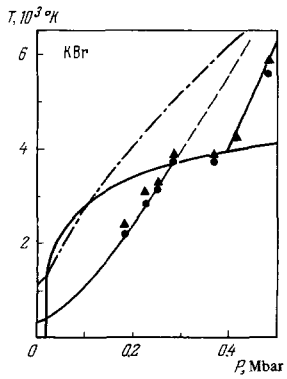

FIG. 26. Phase diagram of KBr [49]. Notation as in Figs. 24 and 25.

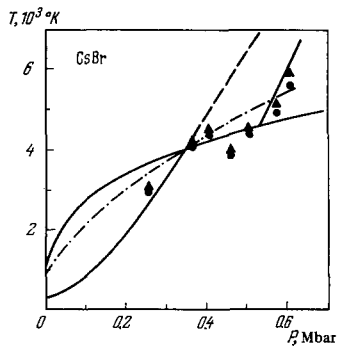

FIG. 27. Phase diagram of CsBr [49]. Notation as in Figs. 24 and 25.

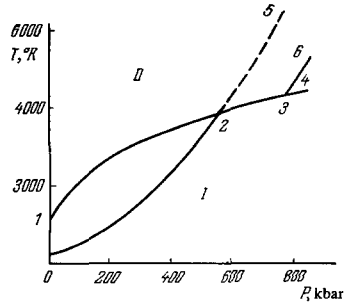

FIG. 28. Shock adiabat in the field of the phase diagram: I – solid phase, II – liquid phase: —— shock adiabat in the solid (0-2) and liquid (4-6) phases, and in the two-phase region (2-3, 4); – – shock adiabat in the superheated solid phase (2-5); melting curve 1-2-3, 4.

Table II

	LiF	NaCl	KCl	KBr	CsBr		LiF	NaCl	KCl	KBr	CsBr
V_0, cm³/g	0.3774	0.4619	0.5015	0.3636	0.2247	L, kJ/g	6.07	1.39	1.29	0.81	0.74
E_0, kJ/g	0.251	0.174	0.147	0.097	0.058	ΔS, J/g deg	1.01	0.38	0.32	0.20	0.16
P_4, kbar	2800	700	480	400	540	$(\Delta S)_0$, J/g-deg	0.929	0.452	0.335	0.210	0.122
T_4, 10^3°K	6.0	3.7	4.1	4.0	4.65	$\Delta V/V_3$, %	3.2	1.6	1.5	2.8	4.5
V_4, cm³/g	0.191	0.255	0.272	0.199	0.128	$(\Delta V/V_3)_0$, %	26	25	19	17	24
V_3, cm³/g	0.185	0.251	0.268	0.194	0.123	dT/dP, deg/kbar	0.6	1.1	1.3	2.8	3.4
E_3, kJ/g	21.9	6.32	4.43	2.80	2.22						

of the shock wave and on the shape of the dynamic adiabat in P-V coordinates. This may explain why melting was always neglected until recently in dynamic investigations of the equations of state of condensed substances. Nevertheless, for a number of materials the presence of melting is actually revealed[129] by a kink on the plot of the shock-wave velocity D against the mass velocity u of the matter behind the wave front. Among these substances are[17,49], e.g., KCl and KBr. However, it is practically impossible to determine the solid-phase boundary from the D(u) plot for NaCl[49]. Van Thiel and Alder[104] determined the transition point of liquid argon into the two-phase region from the kink on the D(u) plot.

Transition to the liquid state may be detected by a change in viscosity, and some results have been already obtained by this method[64,131]. It is important to note that metals on which optical temperature measurements cannot be performed can also be investigated by this method. However, like the inspection of changes in D(u) curves, this method can reveal only the pressure at which melting takes place. In order to find the temperature, i.e., the state in the field of the phase diagram, it is necessary to resort to some equation of state of the investigated substance.

Let us now consider what physical conclusions can be reached through temperature measurements, and first of all the experimental data that characterize the behavior of the solid phase in investigated ionic crystals. It has been shown earlier[49] that in the case of NaCl and KCl the Mie-Grüneisen equation of state, which is a quasiharmonic approximation, describes in a satisfactory manner not only the relationship between pressure and density along a dynamic adiabat but also the temperature of a shock-compressed solid body up to the melting curve, with the specific heat as given by Petit and Dulong. The same applies to KBr and CsBr (see Figs. 26 and 27).

This indicates that the influence of the anharmonic nature of thermal ion oscillation on the specific heat of solid ionic crystals is fairly small. At the same time the experimental data show that the specific capacity of the NaCl lattice is ~10% higher than as given by Petit and Dulong, and that of CsBr is ~5% lower*.

Table II shows the parameters of the states attained behind the front of the shock wave; it can be seen that although the investigated ionic crystals go over into the liquid state at essentially different pressures, but at degrees of compression ($\sigma = V_0/V_4 \approx 1.8$) and at temperatures (about 4 or 5 times higher than the melting points at atmospheric pressure) that are quite close. When ionic crystals are compressed by a factor of about 1.7, they remain solid up to a temperature of about 4000°K, which is much higher than the melting point of the best refractory metals.

Let us now analyze the experimental data obtained when the dynamic adiabat passes into the two-phase (solid and liquid) region (section 2—3 in Fig. 28). Knowing the equation of state for the solid phase and the measured values of pressure, temperature, and density for the point at which the shock adiabat goes from the two-phase into the liquid region, we can calculate the heat of melting at the measured pressure[49] from the following expression

$$L = T_4 \Delta S = E_0 + \frac{1}{2} P_4 (V_0 + V_4 - 2V_3) - E_3, \qquad (14)$$

where E_0 and V_0 are the internal energy and specific volume of the material ahead of the shock front, P_4, V_4 and T_4 are the pressure, specific volume, and temperature of the liquid phase behind the front, and E_3 and V_3 are the internal energy and specific volume of the solid phase at a pressure P_4 and temperature T_4 (the subscripts 3 and 4 are as in Fig. 23). All the initial data, together with the obtained values of heats of melting and entropy and volume jumps, are shown in Table II for the investigated crystals. Estimates show that the accuracy with which ΔS is determined from such measurements is 20—30%. Errors arise mainly as a result of inaccuracies in determination of the specific volume along the dynamic adiabat on the boundaries of the two-phase region. The reliability of the found values of ΔS and ΔV is to some extent supported by the agreement between the experimental and calculated (by the Clausius-Clapeyron equation) slope of the melting curves (see Table II).

Table II permits us to draw several important conclusions. Comparison of $(\Delta S)_0$ and ΔS for low ($P \approx 0$ for LiF, NaCl and CsBr and $P \approx 19$ kbar for KCl and KBr) and high ($P \sim 400$—2800 kbar) pressures indicates that the entropy jump along the melting curves remains nearly constant in all the investigated crystals. This means that the heat of melting increases approximately in proportion to the melting temperature—i.e., by a factor of about 4 or 5 under the investigated conditions.

*See [132] for theoretical estimates.

When the degree of compression is about 1.8, the heat of melting is about 20 to 30% of the total increase in internal energy under shock compression, and 50% of the thermal energy transferred to the material. When $\Delta S \approx$ const, the volume jump occurring on melting decreases very appreciably. Whereas at low pressures $(\Delta V/V)_0 \approx 20\%$, under melting conditions in the shock wave it is only 2–4%. It follows that under strong compression ($\sigma \approx 1.8$) the liquid, at least at the melting point, should differ less in many properties from the solid state than at atmospheric pressure or at pressures of some tens of kilobars.[133] We shall not discuss here the equations of state but only point out that the experimental data made it possible to find[49] separate equations of state for the solid and liquid phases. The melting curve was determined in this case as the boundary between the two phases. The results of such calculations[49], illustrated in Figs. 24–27 (solid lines), describe the phase diagrams of the investigated crystals with sufficient accuracy. The same figures show that the melting curves calculated[49] from the Lindemann-Gilvarry formula[134,135], namely

$$T_m = \text{const} \cdot V^{2/3}\Theta^2 M,$$

[where V is the solid-phase volume on melting, Θ is the Debye temperature, and M is the molecular weight], differ appreciably from experimental data, especially in the cases of KBr and KCl. Contrary to experiment, these curves have a small dT/dP for $P \approx 0$ and a large one when $P \approx 0.5$–1 kbar. Extrapolation of the results of Clark[136] and Pistorious[137] by means of Simon's equation, using their[136,137] coefficients, does not provide a satisfactory description of melting curves at high pressures. In this context let us briefly refer to the discussion recently started between American writers after a communication published by Kraut and Kennedy[138] regarding a new law of melting at high pressures. According to Kennedy[138], in all substances that melt with an increase in volume we have

$$T_m = T_m^0\left(1 + c\frac{\Delta V}{V_0}\right), \qquad (15)$$

where T_m^0 is the melting point at atmospheric pressure, $\Delta V/V_0 = (\delta - 1)\delta$, where δ is the degree of compression of the body along the Bridgman isotherm at a pressure corresponding to T_m, and c is a constant (different for each substance).

Libby[139] maintains that the constant c can be found from the properties of the material at atmospheric pressure. Gilvarry[140] pointed out that Eq. (15) follows from Lindemann's principle, which he used[141] to describe the melting curves at high pressures. Similar results were also obtained by Vaidya and Gopal[142]. We can agree with this only in part, since (15) can be obtained from the Lindemann-Gilvarry equations only for small $\Delta V/V_0$. Beginning from $\Delta V/V_0 \approx 0.1$, in the case of NaCl the relation between T_m and $\Delta V/V_0$ deviates noticeably from a linearity (Fig. 29). We have already pointed out the nature of the difference between melting curves calculated by the Lindemann-Gilvarry equation and the measured curves[49]. Using as an example the melting curve of argon, calculated by the Monte-Carlo method in a wide range of melting points and densities, Ross and Alder[143] have shown that Lindemann's law holds but that Kennedy's equation does not. In a later, more detailed paper[144] Kraut and Kennedy quoted as a proof of the validity of (15) the fact that the data obtained by us[49] for the melting curve of NaCl at high pressures agree with the straight line of (15) with parameters taken from Clark[136] and Pistorious[137] (see Fig. 29). Further checks have shown that a close, but slightly worse, agreement is also found in the case of KCl (Fig. 30) and KBr. Similar comparison of results could not be carried out for CsBr and LiF because of the lack of data at low pressures. Although Kennedy's equation describes fairly well the available measured melting curves of ionic crystals over a wide range of pressures, it apparently cannot be regarded as a melting law, mainly because the melting point and the volume contained in (15) correspond to different states of the substance. This is clearly seen in Fig. 31, which shows in pressure/specific-volume coordinates the Hugoniot adiabat (P_H), the Bridgman isotherm (P_B), and the boundaries of the region of coexistence of two phases (L and S). Kennedy's equation relates the melting temperature at point 1 not to the volume V_1 characterizing the state of the substance at this point, but to volume V_2 corresponding to the body compressed by pressure P_1 along Bridgman's isentropic curve:

$$T_1 = T_0\left(1 + c\frac{V_0 - V_2}{V_0}\right). \qquad (16)$$

On the other hand, if V_1 is substituted for V_2 in (16), the

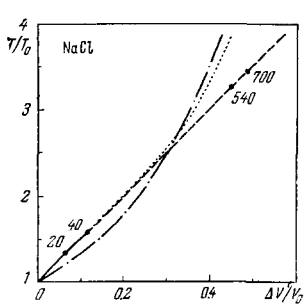

FIG. 29. Comparison of measured and calculated melting curves for NaCl —— measured [136,137]; ● measured [49]; – – calculated [144]; . . . . calculated by Simon's equation with the coefficients taken from [136]; –.– calculated [49] by the Lindemann-Gilvarry equation.

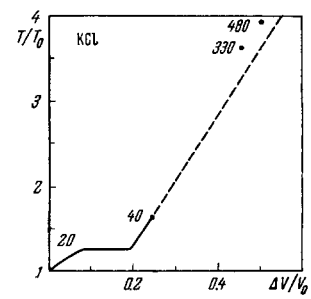

FIG. 30. The same as Fig. 29 but for the case of KCl.

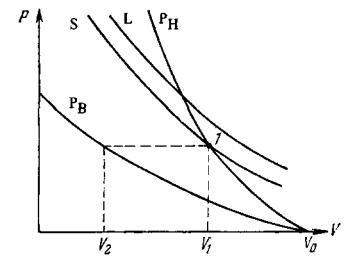

FIG. 31. P-V diagram illustrating how the volume was found by Kraut and Kennedy [144] P_H – Hugoniot adiabat; P_B – Bridgman isotherm. The two-phase (solid and liquid) region lies between the lines S and L.

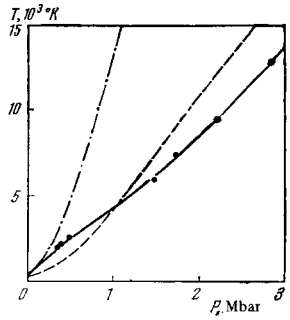

FIG. 32. Temperature of shock-compressed lucite $(C_5H_8O_2)_n$ versus shock-wave intensity ● – measured, – – – calculated taking c_V = 3.74 J/g-deg; –·– calculated taking c_V = 1.22 J/g-deg.

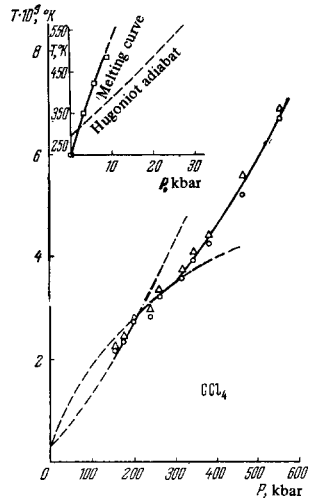

FIG. 33. Temperature of shock-compressed carbon tetrachloride versus shock-wave intensity. Δ, ○ – values measured under shock-compression conditions; □ – measured values [149]; —— interpolation of measured data; – – – extrapolation of measured data.

linear relationship (15) is not valid for ionic crystals over a wide range of pressures[145]. Equation (15) is therefore a nomogram rather than a fundamental law of melting.

9. Measurement of Temperatures of Shock-compressed Lucite and Carbon Tetrachloride

The pressure dependence of the temperature of shock-compressed lucite derived by Sinitsyn, Kirillov, Kuryapin and the present author, is shown in Fig. 32.* If the specific heat of lucite remained the same as under atmospheric pressure (c_V = 1.22 Joule/g-deg), the thermal energy transferred to the body by the shock wave would give rise to substantially higher temperatures (see the dot-dashed line in Fig. 32) than those actually measured. The other limit of the specific heat of lucite can be found by assuming that all atoms have three vibrational degrees of freedom, each having an energy kT (c_V = 3.74 Joule/g-deg). It follows that the specific heat of lucite depends greatly on temperature and density. From investigations at atmospheric pressure it is known (see, e.g.,[148]) that many organic compounds, including polymers, exhibit a substantial rise in specific heat with rising temperature. In this sense the behavior of lucite is similar to that of a substance having a high Debye temperature $\Theta \approx 1500^\circ$K.

To reach a specified temperature at still higher pressures the required thermal energy exceeds the energy of the atomic vibrations. The difference between the two energies increases with rising temperature, and apparently a considerable part of it is spent in breaking the chemical bonds, as has been suggested by Zel'dovich. When P is about 3 kbar, the heat transferred to the lucite should be sufficient to transform the material into carbon (H_2 and O_2 molecules), and even for a partial breakdown of molecular bonds[52]. Some very remarkable results were obtained in studies of carbon tetrachloride. At room temperature and atmospheric pressure this is a liquid ($T_m \cong 250^\circ$K); according to Bridgman[149], it has a melting curve with a fairly high initial (dT/dP) = 0.6×10^{-7} deg/bar. Since at low compressions the temperature increases relatively slowly along the Hugoniot adiabat, even a small pressure should be sufficient to cause transition to the solid state. According to Walsh and Rice[77], this pressure is 2 kbar (Fig. 33). It is obvious that with a further rise of both pressure and temperature under shock compression the Hugoniot adiabat should again reach the region of the liquid phase. The T(P) function along the Hugoniot adiabat, obtained by Kirillov, Grigor'ev and the present writer for carbon tetrachloride, is shown in Figure 33. It can be seen that at a pressure of about 200 kbar CCl_4 undergoes a phase transition associated with absorption of energy. The increase of pressure, and thus of the thermal energy supplied to the body, is accompanied in a certain range of pressures (200 < P < 270 kbar) by a slower temperature rise. This phase transition can be identified with melting of the carbon tetrachloride. Within the framework of this theory, the melting curve can be described by a Simon-type expression:

$$P = A\left[\left(\frac{T}{T_0}\right)^n - 1\right]$$

where A = 4.5 kbar, n = 1.6 and $T_0 = 250^\circ$K; the above expression does not contradict the data of Bridgman[149] or our own (cf. Fig. 33). The entropy jump, found from (14) at P = 270 kbar, exceeds the value of the jump at atmospheric pressure by a factor of about 2. However, there is a possibility that the above change in the nature of the T(P) dependence at pressures of 200–300 kbar may be caused—as in lucite—by chemical breakdown of the carbon tetrachloride with formation of free carbon. It is worth mentioning that the anomaly in the reflectivity of the shock front in CCl_4 begins at the same pressure, about 200 kbar (see Sec. 3).

III. ABSORPTION OF LIGHT BY SHOCK-COMPRESSED IONIC CRYSTALS. ABSORPTION AND CONDUCTION MECHANISM.

10. Experimental Determination of the Absorption Coefficient

Under normal conditions, i.e. at room temperature and atmospheric pressure, single crystals of alkali halides are dielectrics and transmit light in quite a wide range of wavelengths, from 0.2–0.3 to 60–130 μ. Unless special impurities are introduced, the visible light-absorption coefficient α is then about 5×10^{-2} cm^{-1}.

Investigations of the radiation of shock-compressed ionic crystals have shown[49,30] their transparency to be

*Dynamic-compressibility data for lucite [146,147,52] were used to compute and analyze the results.

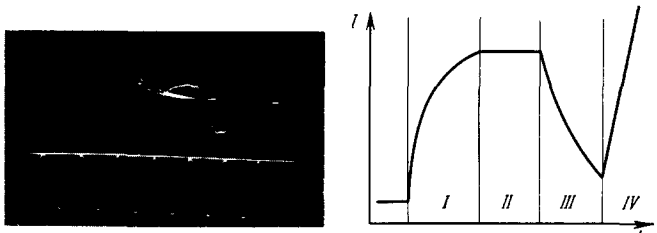

a) b)

FIG. 34. Time dependence of the radiation brightness. a) Oscillogram; b) idealized oscillogram; I – period of increasing brightness; II – period of constant brightness; III – period of decreasing brightness due to decreasing shock-wave intensity: IV – light of shock wave in air.

substantially reduced. This has already been noticed[52] in the case of lucite. A characteristic feature of all these results is that the radiation brightness increases as the shock wave propagates through the investigated body until—at a certain thickness—it becomes constant (see the oscillogram in Figure 34,a). The authors of[49,30], as in[110], ascribe the increase in brightness to an increase in the thickness of the layer compressed by the shock wave and to its transparency. Knowing the time dependence of the radiation brightness, the velocity of the shock wave, and the density behind the shock front, we can find the absorption coefficient of the compressed substance[110,30]:

$$\alpha = \frac{1}{(D-u)\Delta t} \ln \frac{1-I_1/I_2}{I_3/I_2-1}, \qquad (17)$$

where I_1, I_2 and I_3 are the front brightness at the instants t_1, t_2 and t_3; $\Delta t = t_2 - t_1 = t_3 - t_2$; D and u are the wave and mass velocities of the shock wave.

The results illustrated in Fig. 35[30] were obtained in this way. The temperature of the shock-compressed matter (see Sec. 8) and the velocity D of the shock wave were measured[49], and the mass velocities u were found from[15-17] and[49]. The absorption coefficients measured at 6250 and 4780 Å were found to be nearly equal; they exceed the room-temperature values by a factor of 30–100. It is obvious that the absorption coefficient is a function of temperature.

11. Mechanisms of Light Absorption and Conduction in Shock-compressed Ionic Crystals

Light absorption in a solid body is caused by excitation of optical oscillations in the crystal lattice (infrared absorption in ionic crystals), and also by excitation of the electrons. Under normal conditions (atmospheric pressure, T = 300°K) the infrared-absorption band is in the wavelength region of the order of several tens of microns (for NaCl the dispersion frequency is $\nu_0 = 4.9 \times 10^{12}$ sec^{-1}, and for CsBr $\nu_0 = 2.3 \times 10^{12}$ sec^{-1}). Even when we allow for the shift of the infrared-absorption band under compression toward shorter wavelengths[150,30] and for thermal broadening of the absorption band[150-152], we do not arrive[30] at any results comparable to the measured absorption coefficients. Nor can photoexcitation of valence-band electrons explain the measured values of α. If the energy gap were reduced from about 7 or 8 eV to about 2 eV because of the compression and the radiation heating in the shock wave (and such a reduction is required in order for the

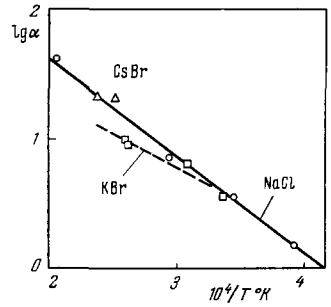

FIG. 35. Temperature dependence of the absorption coefficient α (cm^{-1}) of shock-compressed ionic crystals. O – measured in NaCl[30]; □ – measured in KBr; Δ – measured in CsBr; —, – – interpolation of measured data.

electrons to pass directly into the conduction band in the visible part of spectrum), the values of α would be about 10^4–10^6 cm^{-1}, i.e. 10^3–10^5 times greater than those found by measurement. The obtained results cannot be attributed to indirect optical transitions either, since this would result in a strong wavelength dependence of the absorption coefficient, contrary to the actual observations. One more mechanism of light absorption in ionic crystals can be absorption by color centers. It can be comparable to the measured values, provided the color-center concentration, initially not greater than 10^{14} cm^{-3}, increases sharply under compression to $N \approx 10^7$–10^{18} cm^{-3}. However, in this case the absorption would be selective, contrary to the experimental observations, since the absorption band of the F centers is bell-shaped, with a half-width of about 0.4 eV.

Bearing in mind that the absorption coefficient is little dependent on the wavelength, and is clearly dependent on the temperature, and considering also the above discussion, we must assume[30] that the absorption of light in shock-compressed ionic crystals is caused by intraband transitions of the free electrons. We shall return shortly to the problem of the sources of the free electrons, but at the moment we only note that, within the framework of these ideas, it seems natural to regard also the conduction measured in shock-compressed dielectrics[51,50,15,20] as of electronic nature, caused by the same free carriers[30].

Al'tshuler et al.[15] reached another conclusion. They measured the temperature dependence of the conduction in shock-compressed NaCl and, using the expression $\Sigma \sim \exp(-W_i/kT)$, calculated the activation energy $W_i = 1.2$ eV; from its magnitude, they concluded that the conduction is of ionic character. We recall that under normal conditions $W_c = 1.87$ eV for NaCl, i.e., is 1.5 times as large as the value measured by Al'tshuler et al.[15] When the substance is compressed, the activation energy characterizing the ionic conduction must increase because the ions come closer together, hence the repulsion forces are increased. Let us check this effect numerically. The activation energy for self-diffusion in metals and for ionic conduction in ionic crystals is greater in those crystals that melt at higher temperatures (Figure 36).

The relationship between the activation energy and the melting point can be approximated as follows:

$$W_i \cong 1.6 \cdot 10^{-3} T_m, \qquad (18)$$

where W_i is in eV and T_m in °K.

According to[155] and[156], the activation energy of self-diffusion in all investigated metals increases in

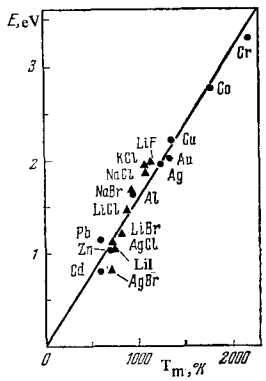

FIG. 36. Activation energy of self-diffusion (ionic conduction) as a function of the melting point at atmospheric pressure. ● – self-diffusion activation energy in metals [153]; ▲ – activation energy of ionic conduction [154].

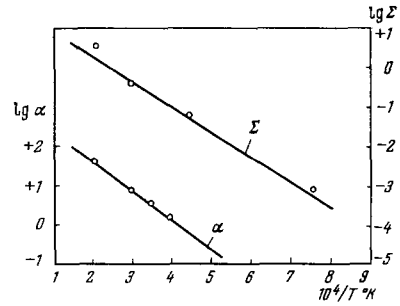

FIG. 37. Conductivity Σ ($ohm^{-1}\,cm^{-1}$) and the absorption coefficient α (cm^{-1}) of NaCl as a function of temperature. O – measured: Σ from [15], α from [30]; —— calculated [30].

proportion to the melting temperature in the measured range of pressures up to 8 kbar. According to the Nernst-Einstein equation, the same dependence should be exhibited by the activation energy of ionic conduction. Analysis of the data reported by Pearce[157], who investigated the dependence of the ionic conduction of NaCl on the applied static pressure (up to 10 kbar), confirms the above conclusion. Hence, as in a variety of substances at atmospheric pressure (Fig. 36), in this material the activation energy increases in proportion to the melting temperature with increasing pressure. This was also the case for the heat of fusion during compression (Sec. 8). Expression (18) can be rewritten as:

$$W_i \cong W_{i,0}\left(\frac{T}{T_0}\right)_m, \tag{19}$$

where $W_{i,0}$ is the activation energy for $P \approx 0$ and $T = 300°K$, T_0 being the melting point under atmospheric pressure ($P \cong 0$). In the compression range of interest to us we have $(T/T_0)_m \approx 3.5-4$ (cf. Sec. 8). The activation energy for the ionic conduction in NaCl thus becomes $W_i = 1.87\ (T/T_0)_m \approx 6-7$ eV, which is about 6 times greater than was found by Al'tshuler et al. Alder[20] also doubted the ionic mechanism of conduction in shock-compressed alkali halides, but thought that the question of the conduction mechanism (ionic or electronic) in alkali halides under shock-compression should be decided by measurements of the Hall coefficient. Our measurements of the absorption coefficient helped us to choose between the two models, and led to the conclusion[30] that both the conduction and light absorption are due to free electrons thermally "ejected" into the conduction band.

Having two independently measured quantities (absorption coefficient α and conductivity Σ), and assuming them to be due to the free carriers, we can find the mobility μ and free-electron concentration N_e. Measurement of one of these quantities, e.g., the conductivity, enables us to find only the product of the carrier concentration and their mobility, since

$$\Sigma = N_e \mu e \tag{20}$$

(e is the electron charge). To find the individual quantities, one usually measures also the Hall coefficient R. The product $R\Sigma = \mu$ gives the mobility. For our purposes, measurement of α is equivalent to measurement of R.

The classical theory relates the absorption coefficient to the free-carrier concentration, the frequency ν of the incident light, and the attenuation factor q (frequency of collisions between electrons and lattice ions) by means of the Drude-Zener equation:

$$\alpha = \frac{2Ne^2}{ncm}\frac{q}{\nu^2+q^2}. \tag{21}$$

In the above, n is the refractive index, c is the velocity of light, m is the effective electron mass (which in our analysis will be taken as the mass of a free electron[158]), and

$$q = \frac{e}{2\pi m\mu}. \tag{22}$$

The mobilities of the free electrons in shock-compressed NaCl, calculated from the experimentally determined conductivity[15] (Fig. 37) and absorption coefficient[30] (Fig. 35), are plotted in Fig. 38 against the measured temperature[49] (see Sec. 8). When the temperature dependence of μ is taken into account, the above values agree well with the data obtained by other authors[159,160].

The dominant factor in ionic crystals is electron scattering by optical lattice vibrations. According to Ziman[161], we then have

$$\mu \approx \frac{3}{\pi^{3/2}2^{9/2}}\frac{n^2}{em^{3/2}c_0}\frac{1}{(KT)^{1/2}}, \tag{23}$$

where $c_0 = 1/\epsilon_\infty - 1/\epsilon_0$, and ϵ_∞ and ϵ_0 are the high-frequency and static dielectric constants. The function μ(T) given by (23), plotted for $c_0 = 0.259$ (which corresponds to ϵ_∞ and ϵ_0 at $T = 300°K$ and $P = 0$), agrees fairly well with the measured values. The agreement is even better when $c_0 = 0.2$ (dot-dash line in Fig. 38).[30] This satisfactory agreement of the calculated electron mobilities with other authors' findings and values calculated with (23) is evidence in favor of the mechanism[30] whereby the light absorption in shock-compressed ionic crystals and their conduction are caused by free electrons. Their concentration (when $T = 3400°K$ and $\sigma = 1.7$) is $N_e = 10^{18}\ cm^{-3}$; the attenuation parameter is then $q \approx 10^{14}\ sec^{-1}$.

Let us now consider the mechanism of the appearance of free carriers in the conduction band. The hypothesis[20] that a thermal transition of the electrons from the valence into the conduction band is made possible because the bands come closer together under compression (narrower energy gap) does not make it possible[30] to describe the measured values of α and Σ in shock-compressed NaCl and their temperature de-

pendences. According to Hamann[162], Drickamer's measurements and the analytical results obtained by Flouer and March[163] speak against the mechanism of narrowing of the energy gap[20]. Because of this, a model was suggested and discussed[30] in which the donor levels, separated by about 2.4 eV from the bottom of the conduction band in NaCl, serve as a source of the free electrons. The above value of 2.4 eV can be found from the Σ (1/T) dependence (see Fig. 37) if the latter is presented as $\Sigma \sim \exp(-W/2kT)$. The required donor density can be found from

$$N_e = N_d^{1/2}\left(\frac{2\pi mkT}{\hbar^2}\right)^{3/4} e^{-W/2kT}, \qquad (24)$$

and if T = 3400°K and σ = 1.7 ($N_e \approx 1.3 \times 10^{18}$ cm^{-3}, W = 2.4 eV) we get $N_d \approx 1.6 \times 10^{19}$ cm^{-3}. This is about 10^5 times greater than the defect (e.g., color-center) concentration characteristic for ionic crystals under normal conditions. It can therefore be concluded that the shock wave is a powerful generator of defects on which electrons are localized. The appearance of such a high defect concentration is quite realistic. Thus, Van Bueren and Kanzaki calculate[164], on the basis of experimental data, that the density of Schottky defects arising in ionic crystals after a 10–35% plastic deformation is 10^{18}–10^{19} cm^{-3}. A number of authors (see, e.g.[165]) have shown that plastic deformation results in the appearance of F-centers. The occurrence of F-centers in shock-compressed MgO was detected by Yager et al.[178]

The above considerations lead to the following mechanism of the effect[30]. When a shock wave propagates through an ionic crystal, the plastic deformation at its front generates defects with electrons localized in them. These defects (most likely, color centers) play the part of donors that dissociate thermally in the shock-heated substance, and this brings free electrons into the conduction band. An initially dielectric ionic crystal is thus transformed by the shock-wave front into a semiconductor with donor levels whose density reaches 10^{19} cm^{-3} in NaCl. The measured conductivities and absorption coefficients in NaCl are quite well described (see Fig. 37) if $N_d = 1.6 \times 10^{19}$ cm^{-3} and W = 2.4 eV. In this model of the considered phenomena, absorption by photoexcitation of electrons localized in the defects should superimpose itself on the absorption due to free carriers. The defect density is quite high, and the contribution of absorption by optical excitation may be appreciable. The maximum of the photoexcitation band should be at energies > 2.4 eV, because the optical gap is wider than the thermal one (see, e.g.,[158]). Measurements in NaCl (at P = 547 kbar) have shown that, when λ = 4000 and 4250 Å the absorption coefficients remain close to their values for λ = 4780 and 6250 Å. This means that the absorption band lies at even higher energies ($h\nu > 3.1$ eV). If we assume that we are dealing here with F-centers, the above is only to be expected, since under normal conditions the maximum of the band in NaCl is at 2.7 eV. Compression by a factor of 1.7 must, according to[166] and[167], bring about a displacement of the maximum of the absorption band into the range of even higher energies, ~4.3 eV.

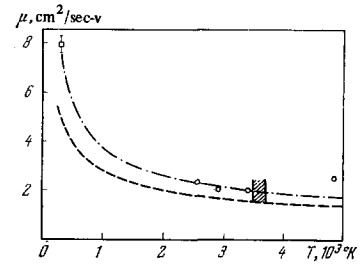

FIG. 38. Free-carrier mobility versus temperature, in NaCl. □ – measurements [159,160]; ○ – measurements [30]; –.– calculations using Eq. (23) [30]. Hatched area = melting zone of shock-compressed NaCl.

We note that the plastic deformation of a body occurring at the shock front causes not only the emergence of defects with localized electrons but also an enormous acceleration of the phase transitions. Thus, for example, whereas in Drickamer's experiments[168] the polymorphic transition in KCl takes several tens of seconds under static pressure, under dynamic pressure the same transition—as shown by the experiments of Al'tshuler et al.[15,169]—requires only 10^{-7} sec, and even 10^{-12} sec when the pressure is higher.[43] A similar difference in the transition times under dynamic[170] and static[171] compression has been found in the case of iron. Such enormous differences in the times (up to 14 orders of magnitude) are evidently due to the production of a great number of defects which accelerate the phase transition process[30]. This is in agreement with the ideas of Alder[20], who associated the reduction in the times of polymorphic transformations under dynamic compression with shear deformations at the shock front.

IV. NONEQUILIBRIUM RADIATION OF SHOCK-COMPRESSED IONIC CRYSTALS

12. Nonequilibrium Radiation at Low Temperatures. Electroluminescence of Shock-compressed Substances

While investigating experimentally the relationship between the temperature of shock-compressed ionic crystals and the pressure, Kirillov, Sinitsyn and this writer found that, in a certain pressure range, the measured light fluxes greatly exceed the values expected at such pressures when the temperatures are calculated with the Mie-Grüneisen equation of state (see Sec. 8). This effect was clearly found for LiF, NaCl,

Table III

Crystal	P, kbar	T, °K (calculated)	T, °K (experimental) λ=0.478 μ	T, °K (experimental) λ=0.625 μ	Crystal	P, kbar	T, °K (calculated)	T, °K (experimental) λ=0.478 μ	T, °K (experimental) λ=0.625 μ
NaCl	270	1250	2440	2270	LiF	340	550	2080	2020
	400	2120	2700	2450		640	1100	2750	2600
CsBr	205	1750	2850	2650		775	1420	3430	3370
	255	2300	3170	3000		1040	2150	3980	3920

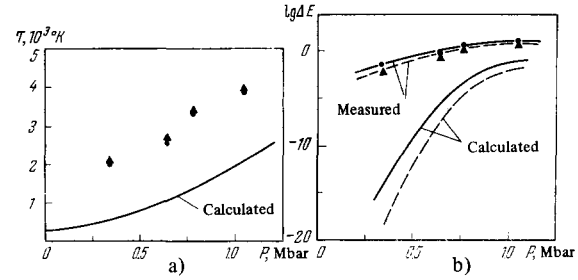

FIG. 39. Comparison of the experimental brightness temperature T(a) and the spectral density of the radiation ΔE (b) of a shock wave in LiF with calculations. ▲ – experimental data for λ = 0.478 μ; ● – experimental data for λ = 0.625 μ.

and CsBr in the pressure range in which the crystals behind the shock front are still solid. Calculated and measured temperatures are compared in Table III.

By experimental temperature is meant here one found from the increased light flux, assuming that the radiation is of the equilibrium type and follows the Planck and Kirchhoff laws (Sec. 7). The listed mental temperatures have, therefore, an arbitrary character, being a measure of the recorded light fluxes. The greatest difference was found in LiF and, moreover, in the widest range of pressures and temperatures). Figure 39 shows the T-P diagram and the density of the light flux ΔE in the spectral range $\Delta\lambda = 100$ Å (Fig. 39,b). It can be seen that when the pressure is 340 kbar the measured value of $\Delta E = 7.65 \times 10^{-3}$ Watt-cm^2 exceeds the expected value by a factor of more than 10^{17}, which is of course far outside any possible experimental error. The observed radiation is certainly not thermal. In fact, the total increase of the internal energy of LiF under shock compression at 340 kbar is 1.5×10^{10} erg/g, and nearly half of it (about 0.65×10^{10} erg/g) is spent in overcoming elastic repulsion forces. If it is assumed that the temperature T = 2080°K corresponds to thermal radiation, then the energy required to heat LiF to this value would be $E_T \approx 4 \times 10^{10}$ erg/g, which is five times as much as the energy supplied in shock compression. It follows from Fig. 39,b that in the entire investigated range of pressures, between 0.34 and 1.04 Mbar in the case of LiF, and at the pressures indicated in Table III for NaCl and CsBr, the luminescence of shock-compressed ionic crystals is of nonequilibrium character. A similar effect was apparently discovered by other workers[172], who studied crystalline quartz shock-compressed along one of its axes, x, normal to the optical axis z. In the shock-compression of fused quartz with pressures of 65, 120 and 265 kbar, and of crystalline quartz along the z and y axes, Brooks[172] observed luminescence spreading from the specimen's periphery toward its center (Fig. 40), which he associated with triboluminescence. It is apparently caused by discharges in cracks that result from lateral unstressing[8] of the shock-compressed quartz. In our case we have a different type of luminescence, for the experiments were carried out in such a way that, as the shock wave traveled through the crystal up to its free surface, the observations were made behind the region not affected by the lateral unstressing. Our data are similar, at least qualitatively, to the results Brooks obtained in crystalline quartz shock-compressed along the x axis, when luminescence starts at once in the entire cross-section of the specimen. This luminescence Brooks[172] regarded as electroluminescence, due either to breakdown of the dielectric or to ionization of NaCl impurities by the electric field generated by the shock wave. The generation of a high-intensity field under shock-compression in quartz[172,32-34], ionic crystals[35-39], and other dielectrics[40,41] is supported by studies in which the appearance of electric current in an external circuit containing no sources of emf was observed. At the same time, according to[30] (see Sec. 11), donor levels with localized electrons appear at the shock front in dielectrics because of plastic deformation. It is therefore possible to disregard the impurities, which Brooks[172] regarded as potential sources of electrons. The combination of a sufficiently strong field (~ 10^5 V/cm) with donor levels acting as electron sources is quite sufficient for carriers to be injected into the conduction band, and to be accelerated there up to optical energies. In this process the electrons have a higher temperature than the lattice. The luminescence is of Planck character, as attested by the weak wavelength dependence of the brightness temperature between 4000 and 6250 Å (Table III). It would be premature to attempt at present a quantitative evaluation of this phenomenon, if only because the mechanism of field generation in shock-compressed dielectrics is still far from clear, and the characteristics of this field are not known either. The theory of this problem is only now being developed[173,174].

FIG. 40. Picture of triboluminescence in shock-compressed quartz at four consecutive instants, according to Brooks [172]. The interval between the photographs is 1.2 μsec.

The observed luminescence can, under certain conditions, be used to produce coherent radiation. According to[175], states with negative temperature may arise when an electric field is switched off very rapidly. With increasing lattice temperature the effects of polarization disappear[38], which indicates a lowering of the field strength, and perhaps its disappearance. On the other hand, the brightness temperature of the luminescence becomes lower than the brightness of thermal radiation. As a result, its effect on the temperatures measured in[49] (see Sec. 8) rapidly disappears with increasing brightness.

13. Nonequilibrium Radiation at High Temperatures. Electronic Screening of the Radiation.

A logical continuation of the studies begun in[49] (cf. Sec. 8) was a move into the pressure range of up to several Mbar, at which the temperatures of shock-compressed alkali halides should reach 1–5 eV. At such temperatures the effect of electrons thrown over from the valence into the conduction band should become noticeable, especially in a crystal like CsBr, which has the smallest energy gap (~ 6 eV). An experimental investigation carried out by Sinitsyn, Kuryapin, and this

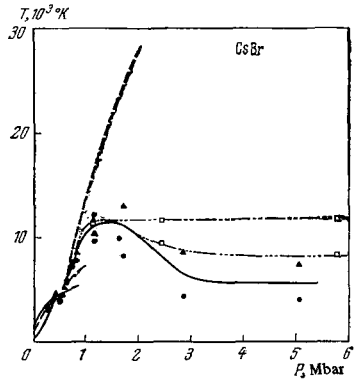

FIG. 41. Brightness temperature of the shock front in CsBr as a function of pressure. ●, ▲ – measured points; —— interpolation of experimental results; – – calculation without allowance for electronic screening; –□– · · – , –□– · · · – calculation with allowance for the electronic screening.

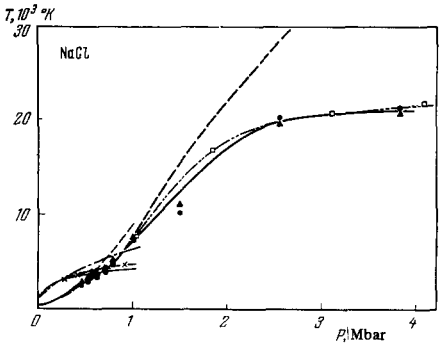

FIG. 42. Brightness temperature of the shock front in NaCl as a function of pressure. [All designations as in Figure 41].

writer yielded a result that was paradoxical at first sight (for details see[179]). The brightness temperature measured in CsBr at P = 5 Mbar was found to be about 0.5 eV, as against around 6 eV expected from the calculations (Fig. 41). Saturation of the brightness temperature, beginning at a certain pressure, was observed in NaCl (Fig. 42), and also in KCl and KBr. A characteristic feature of all these crystals is that the measured temperature is the same as the calculated value up to $T \approx (6-7) \times 10^3$ °K, after which the brightness temperature deviates from the calculated value, saturates, and even becomes lower (in the case of CsBr) as the pressure increases further. In the case of LiF the brightness temperatures are close to the calculated values in the entire range of pressures up to 5 Mbar and temperatures up to about 20×10^3 °K. Summing up the results obtained for five ionic crystals, we can say that the difference between the brightness temperatures and the calculated values increases as the energy gap becomes narrower. Calculations have shown that allowance for the contribution of thermally excited electrons to the specific heat[17] does not produce any great shift of the adiabat in the T-P plane, so that this cannot even begin to account for the measured results. Direct measurement of the reflectivity of the shock front, carried out by the method described in Sec. 1, has shown that the above difference between the measured and calculated temperatures is not caused by a high reflectivity and correspondingly small emissivity of shock-compressed matter. Thus, the measured reflection coefficient in CsBr at P = 1.12 Mbar was R = 4–5%, while to account for the discussed difference in temperatures it would have to be about 60%. With P = 5 Mbar, the necessary value is $R \approx 99\%$, whereas its measured value was $\leq 7\%$. A similar contradiction was also found in other crystals.

The above effect was explained both qualitatively and quantitatively by Zel'dovich, who called attention to the need for taking into account the kinetics of the process in which thermodynamic equilibrium is established between electrons and the lattice.

When a shock wave propagates in a material, the energy supplied to the latter is used up in overcoming elastic interaction forces and in heating the lattice. Since the relaxation times of phonon-phonon interactions are 10^{-12}–10^{-13} sec, the phonon equilibrium temperature Θ is established in this period of time, i.e., in a thickness on the order of 10^{-6} cm. The increase in the electron energy due to electron-phonon interactions causes some electrons to acquire an energy more than double the width of the energy gap. These electrons, having surrendered their energy and passed to the bottom of the conduction band, are capable of ionizing the valence-band electrons and pushing them into the conduction band. This process—shock ionization—increases the concentration of the free electrons. As the electrons absorb energy from the lattice and heat up, the number of hot electrons increases (Fig. 43,b). At this stage (region II in Figs. 43, a and b), the electron temperature does not rise, since all the energy drawn by electrons from the lattice is spent in increasing the number of free electrons by ionization. When the electron concentrations have reached the level at which recombination of the conduction electrons with the holes ($2e^- + e^+ = e^-$) plays a part comparable to that of ionization, the third stage (region III) begins, in which the rate of the increase in the electron concentration is reduced and the energy taken up by electrons from the lattice is spent in raising their temperature. As a result, the electrons reach a state of thermodynamic equilibrium with the lattice (region IV). We are mainly interested in region III, in which the electron temperature has not yet reached the level of the lattice temperature but the electron concentration is already so great that light absorption takes place in a layer thinner than the layer in which equilibrium between electrons and the lattice is reached. In this case we observe a light flux emitted by a certain layer Δ (cf. Fig. 43,a) in which the temperature is still below the equilibrium level, causing the measured temperature to deviate from its true value. That is the qualitative picture of the phenomenon.

Calculations (for details see[180] for CsBr compressed by a shock wave with an amplitude of 5 Mbar have shown that by the time $t \approx 4 \times 10^{-9}$ sec the free

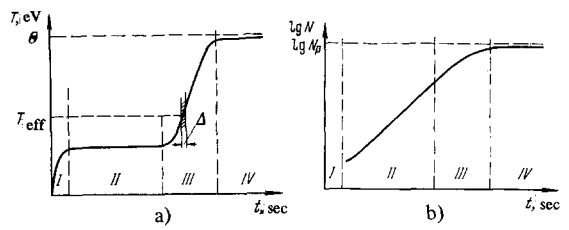

FIG. 43. Qualitative picture of the temperature distribution of the free electrons (a) and their concentration (b) behind the shock front (ordinate). The regions I-IV are defined in the text.

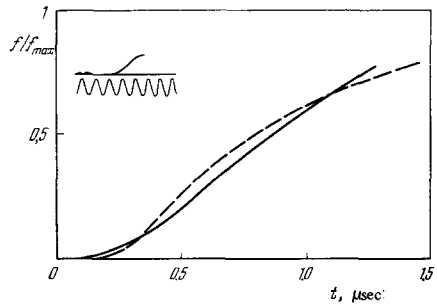

FIG. 44. The rise in the radiation brightness of the shock front in NaCl at P = 465 kbar and Θ = 0.224 eV. —— measured (see oscillogram at the top); — — calculated.

electron concentration reaches $N = 10^{20}$ cm^{-3}. Further fast rise of N makes the absorption coefficient α higher, and the source of the radiation is then a thin layer lagging behind the shock front by about 4×10^{-9} sec. The luminescence of the deeper-lying layers, where the electron temperature reaches its equilibrium value fairly rapidly (in $\Delta t \approx 10^{-9}$ sec), is screened by the forelying layers with $T < \Theta$. The effective temperature is about one-fifth the lattice temperature. The effective temperatures are somewhat higher in NaCl than in CsBr owing to the wider energy gap. Both the measured and the calculated effective temperatures deviate least from the equilibrium value in the case of LiF, even at $P \approx 5$ Mbar, the reason being that the energy gap is relatively wide and Θ is relatively low. These two factors cause a lower density of the free electrons, and consequently a lower degree of screening.

The described mechanism of the phenomenon also explains the low reflectivity at the shock front, in spite of the high electron concentration, 10^{22} cm^{-3}, which is comparable to the free-electron concentration in metals. Even in CsBr, where N is highest, the increase of the free-electron concentration from $N \approx 10^{18}$ cm^{-3}, where it does not affect the reflectivity, to $N \approx 10^{22}$ cm^{-3} takes only 1.4×10^{-9} sec, i.e., it occurs within a layer approximately 1.4×10^{-3} cm thick, while reflection of the incident light requires a small thickness $\Delta \ll 10^{-5}$ cm. In other cases the electron-density gradient is even smaller, so that even the light reflection method, with its high sensitivity to the density gradients, does not make it possible to detect an increase in the free-electron concentration at the shock front.

In conclusion, let us now return to the "low"-temperature region and check the effect of taking into account the kinetics of free-electron generation on the conclusions arrived at in Sec. 11 regarding the absorption and conduction in shock-compressed dielectrics. An analysis carried out for this case, allowing for the fact that the number of electron sources is limited by the donor concentration, has shown that, e.g., in the case of CsBr with $\Theta = 0.4$ eV, the concentration of free electrons in the conduction band and their temperature reach the equilibrium values in a time $t \approx 10^{-8}$ sec. Since $N_e \approx 4 \times 10^{18}$ cm^{-3} and $\alpha \approx 15$ cm^{-1}, the compressed substance remains sufficiently transparent and there is no screening by the electrons. In this case the light flux increases as the shock wave travels through the body, beginning at the instant when thermodynamic equilibrium is established, according to the relation,

$$\frac{f}{f_{\max}} = 1 - \exp(-\alpha l), \tag{25}$$

[f is the light flux radiated by the front ($l = (D - u)t$], which is identical with that considered in Sec. 10.

The only necessary refinement of the picture given in Sec. 10 pertains to the time periods before the electron-lattice equilibrium is established. During those periods the light flux increases rather slowly, because at first N is small and $\alpha \sim N$. Because of this, just after the shock wave has entered the crystal the latter remains transparent, and no radiation can be observed. As N rises exponentially, and α with it, the light flux increases, slowly at first, then faster and faster, until its rate of increase coincides with (25) for α = const. This growth of radiation was observed in our experiments (Fig. 44) in NaCl at P = 465 kbar and Θ = 0.224 eV.

Studies of the radiation in shock-compressed dielectrics provide the experimenter for the first time with means of investigating the kinetics of the thermal excitation of electrons and of the establishment of thermodynamic equilibrium between electrons and the lattice, for in such conditions it is possible to maintain the body in a condensed state at very high temperatures.

[1] L. V. Al'tshuler, Usp. Fiz. Nauk 85, 197 (1965) [Sov. Phys.-Usp. 8, 52 (1965)].

[2] Ya. B. Zel'dovich and Yu. N. Raĭzer, Fizika udarnykh voln i vysokotemperaturnykh gidrodinamicheskikh yavleniĭ [Physics of Shock Waves and High-Temperature Hydrodynamic Phenomena], Moscow, Fizmatgiz, 1963.

[3] M. Rice, R. McQueen and I. Walsh, Solid State Physics, vol. 6, Academic Press, N.Y.-London, 1958.

[4] Ya. B. Zel'dovich, Zh. Eksp. Teor. Fiz. 32, 1577 (1957) [Soviet Phys.-JETP 5, 1287 (1957)].

[5] I. Walsh, M. Rice, R. McQueen and I. Yarger, Phys. Rev. 108, 196 (1957).

[6] L. V. Al'tshuler, K. K. Krupnikov, B. N. Ledenev, V. I. Zhuchikhin and M. I. Brazhnik, Zh. Eksp. Teor. Fiz. 34, 874 (1958) [Sov. Phys.-JETP 7, 606 (1958)].

[7] L. V. Al'tshuler, S. B. Kormer, A. A. Bakanova and R. F. Trunin, ibid 38, 790 (1960) [11, 573 (1960)].

[8] L. V. Al'tshuler, S. B. Kormer, M. I. Brazhnik, L. A. Vladimirov, M. P. Speranskaya and A. I. Funtikov, ibid 38, 1061 (1960) [11, 766 (1960)].

[9] S. B. Kormer and V. D. Urlin, Dokl. Akad. Nauk SSR, 131, 542 (1960) [Sov. Phys.-Dokl. 5, 317 (1960)].

[10] V. N. Zharkov and V. A. Kalinin, ibid, 135, 811 (1960) [5, 1253 (1961)].

[11] S. B. Kormer, V. D. Urlin and L. T. Popova, Fiz. Tverd. Tela 3, 2131 (1961) [Sov. Phys.-Solid State 3, 1547 (1962)].

[12] L. V. Al'tshuler, A. A. Bakanova and R. F. Trunin, Zh. Eksp. Teor. Fiz. 42, 91 (1962) [Sov. Phys.-JETP 15, 65 (1962)].

[13] K. K. Krupnikov, M. I. Brazhnik and V. P. Krupnikova, ibid, 42, 675 (1962) [15, 470 (1962)].

[14] S. B. Kormer, A. I. Funtikov, V. D. Urlin and A. N. Kolesnikova, ibid, 42, 686 (1962) [15, 477 (1962)].

[15] L. V. Al'tshuler, L. V. Kuleshova and M. N. Pavlovskiĭ, ibid, 39, 16 (1960) [12, 10 (1961)].
[16] L. V. Al'tshuler, M. N. Pavlovskiĭ, L. V. Kuleshova and G. V. Simakov, Fiz. Tverd. Tela, 5, 279 (1963) [Sov. Phys.-Solid State 5, 203 (1963)].
[17] S. B. Kormer, M. V. Sinitsyn, A. I. Funtikov, V. D. Urlin and A. V. Blinov, Zh. Eksp. Teor. Fiz. 47, 1202 (1964) [Sov. Phys.-JETP 20, 811 (1965)].
[18] K. K. Krupnikov, A. A. Bakanova, M. I. Brazhnik and R. F. Trunin, Dokl. Akad. Nauk SSR, 148, 1302 (1963) [Sov. Phys.-Dokl. 8, 203 (1963)].
[19] N. Bridgman, in the collection "Solids under Pressure" (ed. by W. Paul and D. Warschauer), New York, 1963.
[20] B. D. Alder: in [19].
[21] D. A. Kirzhnits, Zh. Eksp. Teor. Fiz. 32, 115 (1957) [Sov. Phys.-JETP 5, 64 (1957)].
[22] N. N. Kalitkin, ibid 38, 1534 (1960) [11, 1106 (1960)].
[23] P. DeCarbi and I. Jamieson, Science 133 (No. 3467), 1821 (1961).
[24] W. Libby: Proc. Nat. Acad. Sci. USA, No. 9, 1475 (1962).
[25] G. A. Adadurov, I. M. Barkalov, V. I. Gol'danskiĭ, A. N. Dremin, T. N. Ignatovich, A. M. Mikhaĭlov, V. L. Tal'roze and P. A. Yampol'skiĭ, Dokl. Akad. Nauk SSSR, 165, 851 (1965); Vysokomol. soed. (High Polymers) 7, 180 (1965).
[26] I. M. Barkalov, V. I. Gol'danskiĭ, V. V. Gustov, A. N. Dremin, A. M. Mikhaĭlov, V. L. Tal'roze and P. A. Yampol'skiĭ, Dokl. Akad. Nauk SSSR, 167, 1077 (1966).
[27] L. V. Al'tshuler, I. M. Barkalov, I. N. Dulin, V. N. Zubarev, T. N. Ignatovich and P. A. Yampol'skiĭ, Khimiya vysokikh energiy (High Energy Chem.) 2, 88 (1968).
[28] I. M. Barkalov, V. N. Gustov, I. N. Dulin, V. N. Zubarev, A. G. Kazakevich and P. A. Yampol'skiĭ, Vysokomol. soed., 10, No. 4 (1968).
[29] C. Smith, Memorial de l'artillerie traciaise 35, 463 (1961).
[30] S. B. Kormer, M. V. Sinitsyn, G. A. Kirillov and L. T. Popova, Zh. Eksp. Teor. Fiz. 49, 135 (1965) [Sov. Phys.-JETP 22, 97 (1966)].
[31] F. Neilson, W. Benedick, W. Brooks, R. Graham and G. Anderson, Electrical and Optical Effects of Shock Waves in Crystalline Quartz, Colloque International 1961 sur Les Ondes de Détonation, Paris.
[32] F. Neilson, W. Benedick, Bull. Amer. Phys. Soc. 5, 511 (1960).
[33] R. Graham, F. Neilson and W. Benedick, J. Appl. Phys. 36, 1775 (1965).
[34] R. Graham, J. Appl. Phys. 33, 1755 (1962).
[35] P. Harris, J. Appl. Phys. 36, 739 (1965).
[36] R. Linde, W. Murri and D. Doren, J. Appl. Phys. 37, 2527 (1966).
[37] T. Ahrens, J. Appl. Phys. 37, 2532 (1966).
[38] A. G. Ivanov, V. N. Mineev, E. Z. Novitskiĭ, V. A. Yanov and G. I. Bezrukov, ZhETF Pis. Red. 2, 353 (1965) [JETP Lett. 2, 223 (1965)].
[39] A. G. Ivanov, E. Z. Novitskiĭ, V. N. Mineev, Yu. V. Lisitsyn, Yu. P. Tyunyaev and G. I. Bezrukov, Zh. Eksp. Teor. Fiz. 53, 41 (1967) [Sov. Phys.-JETP 26, 28 (1968)].
[40] D. Fischbach and A. Nowick, J. Phys. Chem. Solids 5, 302 (1958).
[41] G. Hauver, J. Appl. Phys. 36, 2113 (1965).
[42] Ya. B. Zel'dovich, S. B. Kormer, M. V. Sinitsyn and K. B. Yushko, Dokl. Akad. Nauk SSSR, 138, 1333 (1961) [Sov. Phys.-Dokl. 6, 494 (1961)].
[43] S. B. Kormer, K. B. Yushko and G. V. Krishkevich, ZhETF Pis. Red. 3, 64 (1966) [JETP Lett. 3, 39 (1966)].
[44] S. B. Kormer, K. B. Yushko and G. V. Krishkevich, Zh. Eksp. Teor. Fiz. 52, 1478 (1967) [Sov. Phys.-JETP 25, 980 (1967)].
[45] K. B. Yushko, G. V. Krishkevich and S. B. Kormer, ZhETF Pis. Red. 7, 12 (1968) [JETP Lett. 7, 7 (1968)].
[46] Ya. B. Zel'dovich, S. B. Kormer, G. V. Krishkevich and K. B. Yushko, Dokl. Akad. Nauk SSSR, 158, 1051 (1964) [Sov. Phys.-Dokl. 9, 851 (1965)].
[47] Ya. B. Zel'dovich, S. B. Kormer, K. B. Yushko and G. V. Krishkevich, ibid. 171, 65 (1966) [11, 936 (1967)].
[48] P. Bridgman, Proc. Amer. Acad. Arts and Sci. 76, 1 (1945).
[49] S. B. Kormer, M. V. Sinitsyn, G. A. Kirillov and V. D. Urlin, Zh. Eksp. Teor. Fiz. 48, 1033 (1965) [Sov. Phys.-JETP 21, 689 (1965)].
[50] A. A. Brish, M. S. Tarasov and V. A. Tsukerman, ibid. 38, 22 (1960) [11, 15 (1960)].
[51] B. Alder and R. Cristian, Phys. Rev. 104, 550 (1956).
[52] Ya. B. Zel'dovich, S. B. Kormer, M. V. Sinitsyn and A. I. Kuryanin, Dokl. Akad. Nauk SSSR 122, 48 (1958) [Sov. Phys.-Dokl. 3, 938 (1959)].
[53] H. Drickamer, [19].
[54] Modern Very High Pressure Techniques, ed. by R. H. Wentorf, London, 1962.
[55] Physics at High Pressure, Solid State Physics, vol. 11, New York-London, 1960.
[56] D. F. Hornig, Phys. Rev. 72, 178 (1947).
[57] G. R. Gowan and D. F. Hornig, J. Chem. Phys. 18, 1008 (1950).
[58] W. M. Flook and D. F. Hornig, J. Chem. Phys. 23, 816 (1955).
[59] T. I. Ahrens and M. H. Ruderman, J. Appl. Phys. 37, 4758 (1966).
[60] L. H. Jones, W. M. Isbell and C. I. Maiden, J. Appl. Phys. 37, 3492 (1966).
[61] W. Eisenmenger, Acustica 14, 187 (1964).
[62] L. D. Landau and E. M. Lifshitz, Mekhanika sploshnykh sred [Mechanics of Continuous Media]. Fizmatgiz, 1963.
[63] V. L. Ginzburg, Rasprostraneniye elektromagnitnykh voln v plazme [Electromagnetic Wave Propagation in Plasma], Fizmatgiz, 1960.
[64] A. D. Sakharov, R. M. Zaĭdel', V. N. Mineev and A. G. Oleĭnik: Dokl. Akad. Nauk SSSR 159, 1019 (1964) [Sov. Phys.-Dokl. 9, 1091 (1965)].
[65] A. N. Dremin and S. K. Rozanov, ibid 139, 137 (1961).
[66] A. N. Dremin and S. D. Savrov, Fizika goreniya i vzryva (Combustion and Explosion Physics), No. 1, 36 (1966).
[67] K. I. Shchelkin, Zh. Eksp. Teor. Fiz. 36, 600 (1959) [Sov. Phys.-JETP 9, 416 (1959)].
[68] K. I. Shchelkin, Usp. Fiz. Nauk 87, 273 (1961) [Sov. Phys.-Usp. 8, 780 (1966)].
[69] Ya. B. Zel'dovich, Zh. Eksp. Teor. Fiz. 10, 542 (1940).
[70] Yu. N. Denisov and Ya. K. Troshin, Dokl. Akad. Nauk SSSR, 125, 110 (1959).
[71] B. V. Ioffe, Refraktometricheskie metody khimii [Refractometric Methods in Chemistry], GKhI, 1960.

[72] I. L. Fabelinskiĭ, Molekulyarnoye rasseyanie sveta [Molecular Light Scattering], Moscow, Nauka, 1965.
[73] I. F. Rosen, JOSA, 37, 932 (1947).
[74] R. M. Waxler and C. E. Weir, J. NBS, A67, 163 (1963).
[75] R. M. Waxler and C. E. Weir, J. NBS, A68, 489 (1964).
[76] C. V. Raman and K. S. Venkataraman, Proc. Roy. Soc. A171, 137 (1939).
[77] I. M. Walsh and M. H. Rice, J. Chem. Phys. 26, 815 (1958).
[78] M. H. Rice and I. M. Walsh, J. Chem. Phys. 26, 824 (1958).
[79] Handbook of Chemistry and Physics, 37th ed., Cleveland, 1955.
[80] R. M. Waxler and C. W. Weir, J. NBS A69, 325 (1965).
[81] H. Muller, Phys. Rev. 47, 947 (1935).
[82] E. Burstein and P. L. Swith, Phys. Rev. 74, 229 (1948).
[83] P. S. Krishnan, Progr. Crystal Phys., Interscience Publishers, N. Y. 1958.
[84] E. D. D. Schmidt and K. Vedam, Solid State Communs 3, 373 (1965).
[85] E. D. D. Schmidt and K. Vedam, J. Phys. Chem. Solids 27, 1563 (1966).
[86] S. S. Batsanov, Elektrootritsatel'nost' elementov i khimicheskaya svyaz' [Electronegativity of Elements and the Chemical Bond], Novosibirsk, SO AN SSSR, 1963.
[87] K. Vedam and E. D. D. Schmidt, Phys. Rev. 146, 548 (1966).
[88] I. Yamashita, Progr. Theor. Phys. 8, 280 (1952).
[89] I. Yamashita and T. Kurosawa, J. Phys. Soc. Japan 10, 610 (1955).
[90] D. C. Pack, W. M. Evans and H. James, Proc. Phys. Soc. 60 (337), 1 (1948).
[91] M. A. Allen and C. A. McGrary, Rev. Sci. Instr. 24, 165 (1953).
[92] D. Bancroft, E. L. Peterson and S. Minshall, J. Appl. Phys. 27, 291 (1956).
[93] S. Minshall, J. Appl. Phys. 26, 463 (1955).
[94] E. Costello, The Dust. Mech. Engng., Proc. of the Conference on Properties of Materials at High Rates of Strain (London, 1957), 1958.
[95] A. G. Ivanov, S. A. Novikov and V. A. Sinitsyn, Fiz. Tverd. Tela 5, 269 (1963) [Sov. Phys.-Solid State 5, 196 (1963)].
[96] G. R. Fowles, J. Appl. Phys. 32, 1475 (1961).
[97] J. W. Taylor and M. H. Rice, J. Appl. Phys. 34, 364 (1963).
[98] O. E. Jones, F. W. Nellson and W. B. Benedick, J. Appl. Phys. 33, 3224 (1962).
[99] J. Wackerle, J. Appl. Phys. 33 (3), 922 (1962).
[100] A. N. Dremin and T. A. Adadurov, Fiz. Tverd. Tela 6, 1757 (1964) [Sov. Phys.-Solid State 6, 1379 (1964)].
[101] P. W. Bridgman, Amer. Acad. Arts and Sci. 74, 399 (1942).
[102] C. Pistorious, M. C. Pistorious, I. Blakey and L. I. Admiral, J. Chem. Phys. 38, 600 (1963).
[103] L. V. Al'tshuler, A. A. Bakanova and R. F. Trunin, Dokl. Akad. Nauk SSSR 121, 67 (1958) [Sov. Phys.-Dokl. 3, 761 (1959)].
[104] M. Van Thiel and B. Alder, J. Phys. 44, 1056 (1966).
[105] B. Alder and M. Van Thiel, Phys. Lett. 1, 317 (1963).
[106] Udarnye truby [Shock Tubes], Collection of Translations ed. by Kh. A. Rakhmatullin and S. S. Semenov, Moscow, IL, 1962.
[107] Fundamental Data Obtained From Shock-tube Experiments, ed. A. Ferri, 1961.
[108] A. C. Kolb and H. R. Griem, in "Atomic and Molecular Processes", ed. by D. Bates, Interscience, New York, 1962.
[109] R. I. Soloukhin, Udarnye volny i detonatsiya v gazakh [Shock Waves and Detonation in Gases], Fizmatgiz, 1963.
[110] I. Sh. Model', Zh. Eksp. Teor. Fiz. 32, 714 (1957) [Sov. Phys.-JETP 5, 589 (1957)].
[111] A. E. Voĭtenko, I. Sh. Model' and I. S. Samodelov, Dokl. Akad. Nauk SSSR, 169, 547 (1966) [Sov. Phys.-Dokl. 11, 596 (1967)].
[112] J. Roth, J. Appl. Phys. 35 (5), 1429 (1964).
[113] M. N. Alentsev, A. F. Belyaev, N. N. Sobolev and B. M. Stepanov, Zh. Eksp. Teor. Fiz. 16, (11), 990 (1946).
[114] F. Gibson, M. Bowser, C. Summers, F. Scott and C. Mason, J. Appl. Phys. 29, 628 (1958).
[115] I. M. Voskoboĭnikov and A. Ya. Apin, Dokl. Akad. Nauk SSSR, 130 (4), 804 (1960).
[116] V. A. Dement'ev and V. N. Kologrivov, ZhFKh, 36 (3), 458 (1962).
[117] J. Burton and J. Hicks, Nature 202, 758 (1964).
[118] A. N. Dremin and S. D. Savrov, PITF (Appl. and Theor. Phys.), No. 1, 103 (1965).
[119] G. Ribo, Opticheskaya pirometriya [Optical Pyrometry], Gostekhizdat, 1934.
[120] High-Temperature Technology, New York, 1959.
[121] W. Lochte-Holtgreken, Repts. Progr. Phys. 21, 312 (1958).
[122] Ya. B. Zel'dovich and Yu. P. Raĭzer, Zh. Eksp. Teor. Fiz. 35, 1402 (1958) [Sov. Phys.-JETP 8, 980 (1959)].
[123] J. Tailor, J. Appl. Phys. 34 (9) 2727 (1963).
[124] Ya. B. Zel'dovich and Yu. P. Raĭzer, Usp. Fiz. Nauk 63, 613 (1957).
[125] D. Fain, JOSA 55 (4), 460 (1960).
[126] I. Sh. Model', A. Ye. Voĭtenko and F. O. Kuznetsov, PTÉ, No. 6, 121 (1962).
[127] S. G. Grenishin, A. A. Solodovnikov and G. P. Startsev, Photographic Method of Measuring the Temperature of Light Sources. Reports of the Pyrometry Committee of the VNIIM, Collection No. 1, Moscow, Standardgiz, 1958.
[128] M. N. Pavlovskiĭ, V. Ya. Vashchenko and G. V. Simakov, Fiz. Tverd. Tela 7, 1212 (1965) [Sov. Phys.-Solid State 7, 972 (1965)].
[129] V. D. Urlin, Zh. Eksp. Teor. Fiz. 49, 485 (1965) [Sov. Phys.-JETP 22, 341 (1966)].
[130] V. D. Urlin and A. A. Ivanov, Dokl. Akad. Nauk SSSR, 149, 1303 (1963) [Sov. Phys.-Dokl. 8, 380 (1963)].
[131] V. N. Mineev and E. V. Savinov, Zh. Eksp. Teor. Fiz. 52, 629 (1967) [Sov. Phys.-JETP 25, 411 (1967)].
[132] G. Leibfried and W. Ludwig, Theory of Anharmonic Effects in Crystals [Russian translation], IL, 1963.
[133] F. Bundy and H. Strong, Solid State Phys. 13, 81 (1962).
[134] F. Lindemann, Phys. Z. 11, 609 (1910).
[135] J. Gilvarry, Phys. Rev. 102, 308 (1956).

[136] S. Clark, J. Chem. Phys. 31, 1526 (1959).
[137] C. W. Pistorious, J. Phys. Chem. Solids 26, 1543 (1965).
[138] E. Kraut and G. Kennedy, Phys. Rev. Lett. 16, 608 (1966).
[139] W. F. Libby, Phys. Rev. Lett. 17, 423 (1966).
[140] J. Gilvarry, Phys. Rev. Lett. 16, 1089 (1966).
[141] J. Gilvarry, Phys. Rev. 102, 317 (1956).
[142] S. N. Vaidya and E. S. Gopal, Phys. Rev. Lett. 17, 635 (1966).
[143] M. Ross and B. Alder, Phys. Rev. Lett. 16, 1077 (1966).
[144] E. Kraut and G. Kennedy, Phys. Rev. 151, 668 (1966).
[145] S. B. Kormer and V. D. Urlin, ZhETF Pis Red. 8 (1968) [JETP Lett. 8 (1968)].
[146] J. Dagoigny, J. Kieffer and B. Vodar, Compt. rend. 245, 1502 (1957).
[147] A. A. Bakanova, I. N. Dudoladov and R. F. Trunin, Fiz. Tverd. Tela 7, 1615 (1965) [Sov. Phys.-Solid State 7, 1307 (1965)].
[148] P. G. Maslov, Dokl. Akad. Nauk SSSR, 86, 767 (1952).
[149] P. Bridgman, High-Pressure Physics [Russian translation], Gostekhizdat, 1935.
[150] M. Born and Kun Huang, Dynamical Theory of Crystal Lattices, Oxford, 1954.
[151] V. S. Vinogradov, Fiz. Tverd. Tela 4, 712 (1962) [Sov. Phys.-Solid State 4, 519 (1962)].
[152] V. V. Mitskevich, ibid 4, 3035 (1962) [4, 2224 (1963)].
[153] S. D. Gertsriken and I. Ya. Dekhtyar, Diffuziya v metallakh i splavakh v tverdoĭ faze [Diffusion in Metals and Alloys in the Solid Phase], Fizmatgiz, 1960.
[154] C. Kittel, Introduction to Solid-State Physics, Wiley, New York-London, 1956.
[155] N. Nachtrieb, J. Weil, E. Catalano and A. Lawson, J. Chem. Phys. 20, 1189 (1952).
[156] N. Nachtrieb, H. Resing and M. Rice, J. Chem. Phys. 23, 1193 (1955).
[157] C. B. Pearce, Phys. Rev. 123, 744 (1961).
[158] N. Mott and R. Gurney, Electronic Processes in Ionic Crystals, Dover, 1948.
[159] J. Evans, Phys. Rev. 57, 47 (1940).
[160] R. Bube, Photoconductivity of Solids, Wiley, New York-London, 1960.
[161] J. Ziman, Electrons and Phonons, Oxford, 1960.
[162] S. Hamann, Adv. in High-Pressure Research, vol. 1, ed. by R. S. Breadley, Acad. Press, New York, 1966.
[163] M. Flouer and H. March, Phys. Rev. 125, 1144 (1962).
[164] H. Van Bueren, Imperfections in Crystals, 1960.
[165] W. Sabley, Phys. Rev. 133, 1176 (1964).
[166] W. Maish and H. Drickamer, J. Phys. Chem. Solids 5, 328 (1958).
[167] H. Drickamer, in [55].
[168] S. Wiederhorn and H. Drickamer, J. Appl. Phys. 31, 1665 (1960).
[169] L. V. Al'tshuler, M. N. Pavlovskiĭ and V. N. Drakin, Zh. Eksp. Teor. Fiz. 52, 400 (1967) [Sov. Phys.-JETP 25, 260 (1967)].
[170] S. A. Novikov, I. I. Divpov and A. G. Ivanov, ibid. 47, 814 (1964) [20, 545 (1965)].
[171] R. Clendenen and H. Drickamer, J. Phys. Chem. Solids 25, 865 (1964).
[172] W. Brooks, J. Appl. Phys. 36, 2788 (1965).
[173] F. Allison, J. Appl. Phys. 36, 2111 (1965).
[174] Ya. B. Zel'dovich, Zh. Eksp. Teor. Fiz. 53, 237 (1967) [Sov. Phys.-JETP 26, 159 (1968)].
[175] O. N. Krokhin, Dissertation (FIAN, 1962).
[176] S. B. Kormer, K. B. Yushko and G. V. Krishkevich, Zh. Eksp. Teor. Fiz. 54 (6), (1968) [Sov. Phys.-JETP 27 (6), (1968)].
[177] A. J. Bosman and E. E. Havinga, Phys. Rev. 129, 1593 (1963).
[178] W. B. Yager, M. J. Klein and W. H. Jones, Appl. Phys. Lett. (USA) 5, 131 (1964).

Translated by J. Silberstein